NAVAL POSTGRADUATE SCHOOL

MONTEREY, CALIFORNIA

THESIS

UTILIZING MAXIMUM POWER POINT TRACKERS IN PARALLEL TO MAXIMIZE THE POWER OUTPUT OF A SOLAR (PHOTOVOLTAIC) ARRAY

by

Christopher Alan Stephenson

December 2012

Thesis Advisor:	Sherif Michael
Second Reader:	Robert Ashton

Approved for public release; distribution is unlimited

THIS PAGE INTENTIONALLY LEFT BLANK

REPORT DOCUMENTATION PAGE		Form Approved OMB No. 0704-0188

1. AGENCY USE ONLY *(Leave blank)*	2. REPORT DATE December 2012	3. REPORT TYPE AND DATES COVERED Master's Thesis

4. TITLE AND SUBTITLE Utilizing Maximum Power Point Trackers in Parallel to Maximize the Power Output of a Solar (Photovoltaic) Array	5. FUNDING NUMBERS
6. AUTHOR(S) Christopher A. Stephenson	
7. PERFORMING ORGANIZATION NAME(S) AND ADDRESS(ES) Naval Postgraduate School Monterey, CA 93943-5000	8. PERFORMING ORGANIZATION REPORT NUMBER
9. SPONSORING /MONITORING AGENCY NAME(S) AND ADDRESS(ES) N/A	10. SPONSORING/MONITORING AGENCY REPORT NUMBER

11. SUPPLEMENTARY NOTES The views expressed in this thesis are those of the author and do not reflect the official policy or position of the Department of Defense or the U.S. Government. IRB Protocol number: N/A.

12a. DISTRIBUTION / AVAILABILITY STATEMENT Approved for public release; distribution is unlimited	12b. DISTRIBUTION CODE

13. ABSTRACT (maximum 200 words)

It is common when optimizing a photovoltaic (PV) system to use a maximum power point tracker (MPPT) to increase the power output of the solar array. Currently, most military applications that utilize solar energy omit or use only a single MPPT per PV system. The focus of this research was to quantify the expected benefits of using multiple MPPTs within a PV system based on current technologies and to summarize what may be possible in the near future. In this thesis, the advertised 5-8% gains in efficiency claimed by manufacturers of the multiple MPPT approach were tested and a set of generalized recommendations concerning which applications may benefit from this distributed approach, and which ones may not were sought. The primary benefit of utilizing multiple MPPTs is the concept that independently operating panels within a solar array could increase the overall reliability and resiliency of the entire PV system and potentially allow for solar applications to be used in particularly harsh and dynamic environments with increased confidence. Additionally, using multiple, smaller MPPTs could decrease the overall array dimensions that would save space, reduce weight, and lower costs.

14. SUBJECT TERMS Solar Efficiency, Maximum Power Point Tracker, Micro-inverter, Micro-converter, Power Optimizer, Distributed Solar Array	15. NUMBER OF PAGES 137
	16. PRICE CODE

17. SECURITY CLASSIFICATION OF REPORT	18. SECURITY CLASSIFICATION OF THIS PAGE	19. SECURITY CLASSIFICATION OF ABSTRACT	20. LIMITATION OF ABSTRACT
Unclassified	Unclassified	Unclassified	UU

NSN 7540-01-280-5500 Standard Form 298 (Rev. 2-89)
Prescribed by ANSI Std. 239-18

THIS PAGE INTENTIONALLY LEFT BLANK

Approved for public release; distribution is unlimited

UTILIZING MAXIMUM POWER POINT TRACKERS IN PARALLEL TO MAXIMIZE THE POWER OUTPUT OF A SOLAR (PHOTOVOLTAIC) ARRAY

Christopher A. Stephenson
Captain, United States Marine Corps
B.A., United States Naval Academy, 2003

Submitted in partial fulfillment of the
requirements for the degree of

MASTER OF SCIENCE IN ELECTRICAL ENGINEERING

from the

NAVAL POSTGRADUATE SCHOOL
December 2012

Author: Christopher A. Stephenson

Approved by: Sherif Michael
Thesis Advisor

Robert Ashton
Second Reader

R. Clark Robertson
Chair, Department of Electrical and Computer Engineering

THIS PAGE INTENTIONALLY LEFT BLANK

ABSTRACT

It is common when optimizing a photovoltaic (PV) system to use a maximum power point tracker (MPPT) to increase the power output of the solar array. Currently, most military applications that utilize solar energy omit or use only a single MPPT per PV system. The focus of this research was to quantify the expected benefits of using multiple MPPTs within a PV system based on current technologies and to summarize what may be possible in the near future. In this thesis, the advertised 5–8% gains in efficiency claimed by manufacturers of the multiple MPPT approach were tested and a set of generalized recommendations concerning which applications may benefit from this distributed approach, and which ones may not were sought. The primary benefit of utilizing multiple MPPTs is the concept that independently operating panels within a solar array could increase the overall reliability and resiliency of the entire PV system and potentially allow for solar applications to be used in particularly harsh and dynamic environments with increased confidence. Additionally, using multiple, smaller MPPTs could decrease the overall array dimensions that would save space, reduce weight, and lower costs.

THIS PAGE INTENTIONALLY LEFT BLANK

TABLE OF CONTENTS

THIS PAGE INTENTIONALLY LEFT BLANK

LIST OF FIGURES

THIS PAGE INTENTIONALLY LEFT BLANK

LIST OF TABLES

THIS PAGE INTENTIONALLY LEFT BLANK

LIST OF ACRONYMS AND ABBREVIATIONS

AC	Alternating Current
CCM	Continuous Conduction Mode
CMOS	Complementary Metal-Oxide Semiconductor
CV	Constant Voltage
DC	Direct Current
DCM	Discontinuous Conduction Mode
DoD	Department of Defense
FF	Fill Factor
EHP	Electron-Hole-Pair
I_{SC}	Short Circuit Current
I-V	Current Voltage
MPP	Maximum Power Point
P_{IN}	Input Power
MPPT	Maximum Power Point Tracker
PN	P-type, N-type
P&O	Perturb and Observe
P_{OUT}	Output Power
PV	Photovoltaic
P-V	Power Voltage Curve
UAV	Unmanned Aerial Vehicle
VO	Electric Field
V_{OC}	Open Circuit Voltage

THIS PAGE INTENTIONALLY LEFT BLANK

EXECUTIVE SUMMARY

In the past few years, the U.S. Department of Defense (DoD) has launched numerous initiatives to become more energy efficient and to rely on alternative energies such as biomass, hydropower, geothermal, wind, and solar to reduce their dependence on fossil fuels. In order to set goals and coordinate energy issues, each branch of the nation's armed forces has translated this DoD mandate into formal policies and working groups to include the Army Energy Security Implementation Strategy, the Navy's Task Force Energy, the Air Force Energy Plan, and the Marine Corps' Expeditionary Energy Office [1]. Each service is particularly interested in using solar energy to extend the operational performance of tactical electronic systems and to decrease the military's reliance on disposable batteries. This is typically accomplished through the use of photovoltaic (PV) systems that may include a maximum power point tracker (MPPT) with power conversion capabilities to further improve the performance of solar arrays. The focus of this thesis is on the benefits and limitations of using multiple MPPTs within a PV system, and general recommendations regarding the type of DoD applications that would benefit the most from their use are provided.

In order to achieve a higher efficiency, an MPPT detects and tracks a solar array's maximum power point (MPP). However, the array's MPP is not constant or easily known; this is due to the nonlinear relationship between a cell's output and input variables (i.e., solar irradiation and temperature) which results in a unique operating point

along the current-voltage (I-V) curve where maximum power is delivered [2]. When a PV array is connected directly to the load, referred to as a directly-coupled system, the overall operating voltage of the system is determined by the intersection of the load line and I-V curve and rarely coincides with the MPP as shown in Figure 1 [3]. An MPPT ensures the PV system provides maximum power by allowing the array to operate independently from the load. The MPPT samples the output and properly loads the array to operate at the MPP despite fluctuating environmental conditions.

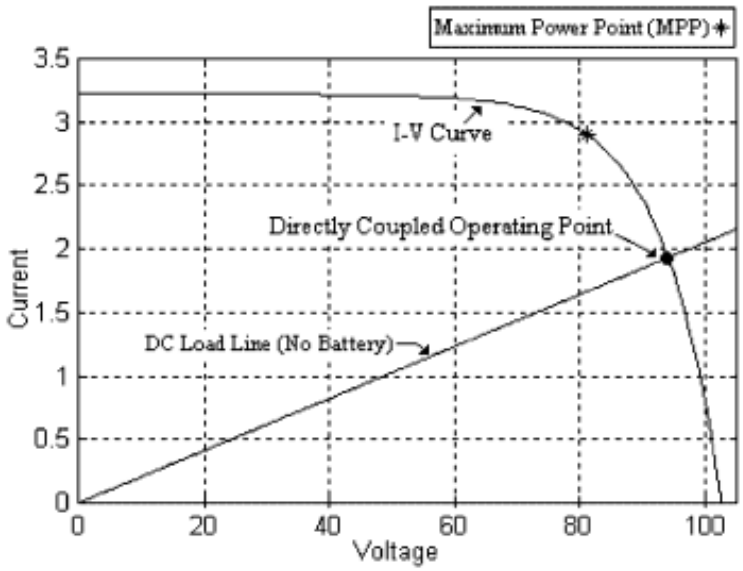

Figure 1. The I-V curve of a PV system with MPP and direct-loading operating points depicted (From [4]).

Historically, MPPTs were large and expensive, and their use was typically limited to large-scale, terrestrial applications comprised of relatively homogenous panels being exposed to similar environmental conditions (i.e., a solar farm). For these reasons, a single MPPT, called a

central converter/inverter, was placed prior to the load and controlled the operating point of the entire solar array. However, within the last few years, numerous engineering and economic factors have made it possible to drastically decrease the size and cost of MPPTs while improving their efficiency. This synchronization of price and performance has also coincided with a rapid, world-wide demand for solar energy within the past 10 years. In 2008, the PV industry began to see companies attempt to market the multiple MPPT concept by selling small, inexpensive MPPTs with inverters that are designed to be installed on each panel of a larger array. Advertised gains in efficiency are between 5–8% for both direct current applications (i.e., micro-converters or power optimizers) and alternating current applications (i.e, micro-inverters) [5].

In addition to the gain in efficiency, assigning an MPPT to each panel within an array results in numerous benefits to include:

- Higher reliability–Since micro-converters are not subjected to as high power and heat loads, they last longer. Manufacturers typically offer warranties of 20–25 years for micro-converters and 10–15 years for a larger array converter.
- Flexibility in future requirements–Expansion of the micro-converter system is cost effective since each panel operates independently.
- Distributed approach–Micro-converters prevent localized disruptions from affecting the entire system. If something is wrong with a solar panel or the corresponding micro-converter, the rest of the system is unaffected.
- Safety–Directly-coupled or single MPPT applications typically require higher voltage

wiring to handle the 300-600 V direct current voltage potential. Micro-converters improve safety by eliminating the need for high voltage wiring since each panel inverts the power, and the output is tied to the commercial grid.

The focus of this research was to quantify the expected benefits of using multiple MPPTs based on current technologies and to summarize what may be possible in the near future. Additionally, a set of generalized recommendations is desired concerning which applications may benefit from multiple MPPTs and which ones are better suited for a central converter or direct loading approach. The anticipated benefits of utilizing multiple MPPTs include a decrease in overall array dimensions that would save space, reduce weight, and lower costs. Additionally, panels that operate independently could increase the overall reliability and resiliency of the entire PV system and potentially allow for solar cells to be used in particularly harsh and dynamic environments with increased confidence.

The expected efficiency gains of using multiple MPPTs were experimentally tested by subjecting a multi-panel solar array to varying levels of irradiance in different system configurations. Varying the levels of irradiance was accomplished by independently tilting the arrays at approximated angles from the sun. For each irradiance level, three tests configurations were implemented to include direct-loading, central converter and micro-inverter scenarios, and the relevant input and output voltages and currents were recorded. The results of these experiments lead to the conclusion that for all irradiance levels, the central converter and micro-inverter approach

outperformed direct-loading. Additionally, it was shown that the micro-inverter approach excelled when the panels were exposed to drastically different levels of irradiance. This is in contrast to when the panels experienced similar levels of irradiance, and virtually no benefit was found in using micro-converters vice a central converter. Finally, a general observation was made that MPPTs are not as effective when used with lower quality solar cells (i.e., those with a poor fill factor) due to the linear nature of their I-V curves.

Based on the results of these tests, recommendations about the use of multiple MPPTs can be made to the PV system designer. First, multiple MPPTs excel when portions of the array are being subjected to a dynamic range of input conditions. Second, multiple MPPTs should be used when a degree of resiliency is desired in the system. In other words, by operating independently, degradation or failure of one panel does not disproportionately affect the performance of the entire array. Finally, multiple MPPTs should be used when system longevity is a primary concern or when access to the array is difficult. Smaller MPPTs typically outlast larger MPPTs and can extend the service life of specialized applications such as satellite systems.

The Army and the Marine Corps are particularly interested in lightening the load of the modern soldier. Each branch of the armed forces would also benefit from a light-weight and efficient technology that maximizes the flight time of their small to medium sized unmanned aerial vehicles. Both of these examples are military applications

that experience a dynamic range of environmental conditions that could possibly benefit from this research.

EXECUTIVE SUMMARY REFERENCES

[1] ***DoD's energy efficiency and renewable energy initiatives,*** Environmental and Energy Study Institute, Washington, DC 2011 [Online]. Available: http://files.eesi.org/dod_eere_factsheet_072711.pdf. Accessed 19 Novemeber 2012

[2] J. Jiang et al., "Maximum power point tracking for PV power systems," in ***Tamkang Journal of Science and Engineering***, Vol. 8, No. 2, 2005 pp. 147–153.

[3] D. Hettelsater et al. (2002, May 2). ***Lab 7: solar cells*** [Online]. Available: http://classes.soe.ucsc.edu/ee145/Spring02/EE145Lab7.pdf

[4] A. D. Gleue. (2008, June). ***The basics of a photovoltaic solar cell*** [Online]. Available: http://teachers.usd497.org/agleue/Gratzel_solar_cell%20assets/Basics%20of%20a%20Photovoltaic%20%20Solar%20Cell.htm

[5] ENPHASE. (2012, November 9). ***Micro-inverter energy performance analysis*** [Online]. Available: http://enphase.com/wp-uploads/enphase.com/2011/08/Enphase-Handout-Performance-versus-PVWatts.pdf

THIS PAGE INTENTIONALLY LEFT BLANK

ACKNOWLEDGMENTS

My initial gratitude is extended to my thesis advisor, Dr. Sherif Michael, for his experience and advice in the formulation of this topic and the guidance provided throughout this research. Your enthusiasm for teaching has made this process an enjoyable experience. Additionally, my second reader, Dr. Robert Ashton, provided me with the necessary knowledge to understand converter technologies and troubleshoot any initial difficulties with the commercial hardware myself. Although Dr. Ashton's power conversion expertise was not utilized to the fullest due to the goals of this research changing, I appreciate his willingness to take on the role of second reader.

I would also like to thank Dr. James Calusdian, Mr. Jeff Knight, and Mr. Warren Rogers for always being available for advice and helping me complete this research.

I would also like to specifically recognize the efforts of Mr. Ron Phelps in the Space Systems Academic Group. Quite simply, the hardware challenges I faced could not have been solved without his help. The additional hours spent by Mr. Phelps getting the solar simulator running, soldering minuscule resistors on to boards, and countless other activities is deeply appreciated. The fact that he graciously accepted this increased workload for an out-of-department student speaks volumes.

My wife gets the final thank you. There were more than a few long days both in the pursuit of this thesis and completing the academic workload at NPS. Taking care of two toddlers all day, every day, is not an easy task. You make

it seem effortless and I appreciate your support and resulting contribution to this endeavor.

I. INTRODUCTION

A. BACKGROUND

A maximum power point tracker (MPPT) is an optimizing circuit that is used in conjunction with photovoltaic (PV) arrays to achieve the maximum delivery of power from the array to the load. Modern MPPTs typically include a microcontroller that is responsible for detecting the maximum power point (MPP) and a power converter/inverter that ensures the array output satisfies the load requirements (i.e., a specific battery charging profile).

The usage of MPPTs has been well established for large-scale, terrestrial PV applications. The placement of a single MPPT at the output of a relatively homogeneous PV system forces the panels to operate near their maximum power efficiency by matching the impedance of the source with the load. In other words, the MPPT forces the panel to operate at a specific voltage and current based on load requirements with consideration to non-linear input variables such as solar irradiance levels, angle of incidence, and temperature. The application of multiple MPPTs at the individual panel level has typically been avoided given the size, conversion inefficiencies, and high-cost of early MPPTs. However, in the last 10 years, MPPTs with direct current (DC) converters and alternating current (AC) inverters have become relatively inexpensive and small in size. This has led to the increased usage of MPPTs in PV applications where size and weight are of great concern; specific examples include the military's interest in reducing the tactical load and logistical requirements

of deployed personnel and the aerospace industry's desire to extend the service life of satellites or increase the range of unmanned aerial vehicles (UAVs).

Commercial vendors are beginning to market the use of multiple MPPTs as power optimizers or micro-converters for DC applications and micro-inverters for AC applications. These two technologies are forecasted to grow rapidly and will compromise 10% of the inverter market by 2016 with revenues of nearly $1.5 billion [1].

B. OBJECTIVES

This objective of this research is to quantify the increase in efficiency of a multiple-panel PV system by allocating individual MPPTs with DC converters to each panel. Applications best suited for multiple MPPTs are also considered and recommendations for usage based on present and near-future technologies are provided. Finally, the possibility of integrating MPPTs with converters for each individual solar cell in a system will be analyzed, and recommendations to achieve optimal efficiency in a cost-efficient and realistic manner will be provided.

C. SCOPE, ORGANIZATION, AND METHODOLOGY

1. Scope and Organization

The scope and organization of this research will include:

- Basic overview and history of solar cells.
- Basic overview of MPPTs to include various tracking algorithms.
- Building the case for the usage of multiple MPPTs.

- Presentation of the data obtained during the testing of a multiple-panel array with and without MPPTs under varying irradiance conditions.
- General observations and conclusions of the data gathered.
- Recommendations to the type of environments multiple MPPT technology may be beneficial.
- Recommendations for future research.

2. Methodology

The research methodology will consist of:

- A literature review of academic publications, trade journals, commercial solutions, relevant research publications, and Internet-based materials.
- Experimental testing in a controlled environment of commercially purchased MPPTs that are representative of the current technology available to a PV system engineer.

3. Related Work

Assigning more than one MPPT per PV system is a relatively new technology for the solar industry. This statement is not meant to suggest that the concept of using an MPPT is new. MPPTs have been studied and experimented with extensively and the benefits are well known, both in academia and the commercial sector. But as a general rule, the bulky size and expense of traditional MPPTs have made them only practical for large-scale, terrestrial applications. However, within the last few years, numerous engineering and economic factors have made it possible to drastically decrease the size and cost of MPPTs while improving their efficiency. This synchronization of price and performance has also coincided with a rapid, world-wide

demand for solar energy within the past 10 years. In 2008, the PV industry began to see companies attempt to market the micro-inverter concept by selling small, inexpensive MPPTs with inverters that are designed to be installed on each panel of a larger array.

There is very little independent validation that the use of more than one MPPT per array is beneficial. Companies that sell micro-inverters claim that for a relatively nominal cost, customers can expect between five and 25% improvements in output power depending on numerous variables. This statement is quite significant considering improvements in solar cell technology is usually minor and typically comes at a considerable expense. The "numerous variables" that affect the power output of an array using multiple MPPTs will also be further explored.

D. EXPECTED BENEFITS

In an ideal PV system, each individual solar cell should have an MPPT assigned to it that compensates for the numerous factors that degrade overall system performance. These factors could include quality-control challenges that result from the mass-manufacturing process of solar cells, environmental conditions such as changing irradiance levels while deployed, or cell failure/degradation due to physical damage or age. This ideal, per-cell application of MPPTs must be balanced with the reality that additional components increases cost, occupies space, adds weight, introduces reliability concerns, and often requires power to operate. The focus of this research is to quantify the expected benefits of using multiple MPPTs based on current technologies and summarize what may be possible in the near

future. Specifically, the point of diminishing return will be related to certain PV applications in order to provide a generalized set of recommendations in the implementation of this concept. The anticipated benefits of maximizing the solar power output of an array include a decrease in overall array dimensions that would save space, reduce weight, and lower costs. Additionally, panels that operate independently could increase the overall reliability and resiliency of the entire PV system and potentially allow for solar cells to be used in particularly harsh and dynamic environments with increased confidence. The emergence of small, power efficient MPPTs are a relatively new technology and may significantly change how the solar industry currently employs them. A better understanding of relevant solar applications that could benefit the most from their use will be provided by this research.

THIS PAGE INTENTIONALLY LEFT BLANK

II. SOLAR CELL BASICS

A. HOW A BASIC SOLAR CELL IS CREATED

1. The p-Type n-Type (p-n) Junction

A solar cell, or p-n junction, is created when two semi-conductor materials with opposing charges are brought in contact with each other. One side, designated as a p-type semiconductor (p for positive), has an excess of holes. The other side has an excess number of electrons and is designated as the n-type semiconductor (n for negative). When the two materials are brought into contact, the excess holes begin to diffuse toward the n-side, and the excess electrons diffuse to the p-side. Eventually, the diffusion of holes and electrons reaches an equilibrium point, and a charge-free region vacant of any electrons and holes is formed between the two semi-conductors. This region is referred to as the depletion region and consists of ionized acceptor atoms on the p-side and donors on the n-side. Figure 1 is an illustration of a typical p-n junction and the resulting electric field V_o that is created by the depletion region.

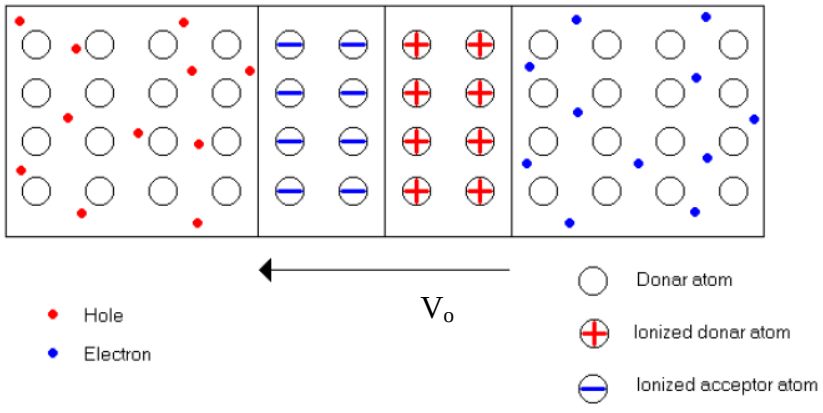

A depiction of the p-n junction (After [2]).

The presence of the electric field causes the electrons and holes to experience an opposing electrical force called drift current. Equilibrium occurs when the drift current J_{Drift} is equal to the diffusion current J_{Diff} which results in a net current flow of zero. The total current density for the electrons or holes is described by

$$\begin{aligned} J_{nTotal} &= J_{nDrift} + J_{nDiff} \\ J_{pTotal} &= J_{pDrift} + J_{pDiff} \end{aligned} \tag{2-1}$$

where J_{Total} is the summation of the drift and diffusion currents. The individual current densities are given by

$$\begin{aligned} J_n &= qnu_n E + qD_n \frac{dn(x)}{dx} \\ J_p &= qpu_p E + qD_p \frac{dn(x)}{dx} \end{aligned} \tag{2-2}$$

where n and p are electron and hole concentrations, μ is the drift mobility, E is the electric field, and $D_{n,p}$ are the diffusion coefficients [2].

2. Forward Bias

Applying a positive voltage to the p-type semiconductor causes a net current flow in the positive direction. A p-n junction under forward bias conditions is depicted in Figure 2.

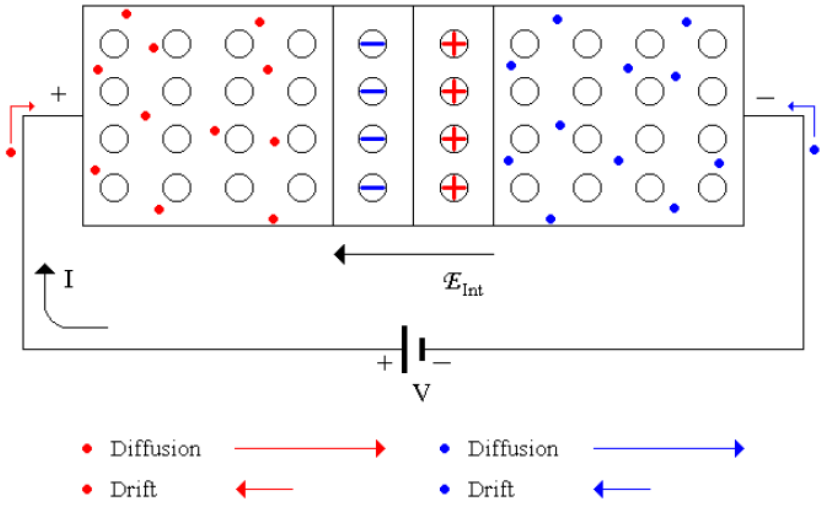

Figure 2. Forward biasing of a p-n Junction (From [2]).

The applied voltage V opposes the internal electric field contained in the depletion region and reduces the potential barrier by the quantity $V - V_o$. Reducing the barrier allows for majority charge carriers to travel across the depletion region by a factor of $e^{(qV/kT)}$ where q is the charge of an electron in coulombs, k is Boltzmann's constant, and T is the temperature in Kelvin. Once these majority charge carriers enter the opposing material they become minority charge carriers. This process is referred to as minority carrier injection and allows the diffusion current to dominate the p-n junction when subjected to a forward bias condition. The diffusion current I_{diff} under these conditions can be described by

$$I_{diff} = \left| I_{drift} \right| e^{qV/kT} \qquad (2\text{-}3)$$

where I_{drift} is the drift current. The total current of a p-n junction under forward bias is simply the diffusion current

minus the absolute value of the opposing drift current I_0. The total current I is given by

$$I = I_0\left(e^{qV/kT} - 1\right) \tag{2-4}$$

which is also known as the ideal diode equation. Finally, a more accurate diode equation can be found by substituting the individual diffusion currents into Equation (2-4) and solving for the minority injection currents to give

$$I = qA\left(\frac{D_p}{L_p}p_n + \frac{D_n}{L_n}n_p\right)\left(e^{qV/kT} - 1\right) \tag{2-5}$$

where $L_{p,n}$ are the diffusion lengths of the holes and electrons, p_n and n_p are the minority charge concentrations, and A is the area of the device.

3. Solar Radiation to Electric Energy

Each light photon that is absorbed by a semiconductor that exceeds the material's band gap has the potential to generate an electron-hole pair (EHP). If the minority carrier that results from an EHP diffuses towards the depletion region, it will be swept to the opposite side by the internal field. This will cause the drift current to increase and a build-up of holes on the p-type semiconductor and electrons on the n-type semiconductor. This results in a forward bias condition for the p-n junction, and the same diode current equations described in Equations (2-4) and (2-5) can be used. The excess majority charge carriers diffuse away from the depletion region and oppose the diode current. The diffusion current is now referred to as the photogeneration current I_{Ph}, and if an

external load is connected, it can be utilized to perform electrical work. As shown in Figure 3, the excited electrons travel along the completed pathway giving up part of its extra energy as electrical power and then return to recombine with the holes via the back contact [2].

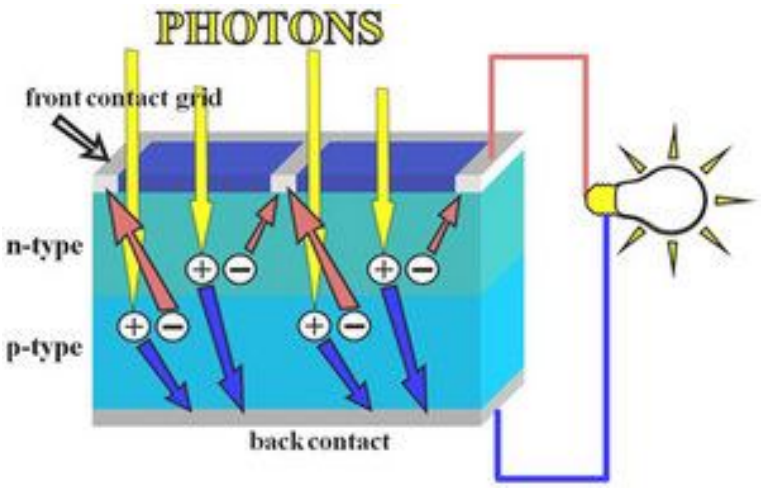

Figure 3. The generation of photocurrent in a solar cell (From [3]).

B. SOLAR CELL PARAMETERS

Solar cells are characterized by their open circuit voltage (V_{OC}), short circuit current (I_{SC}), efficiency (η), and cell quality referred to as the fill factor (FF).

1. Open Circuit Voltage

Under open circuit conditions, each side of the p-n junction allows for a buildup of charge creating a diode current. Once the diode current equals the opposing I_{Ph}, the device is in equilibrium. Figure 4 is a depiction of a solar cell under open circuit conditions.

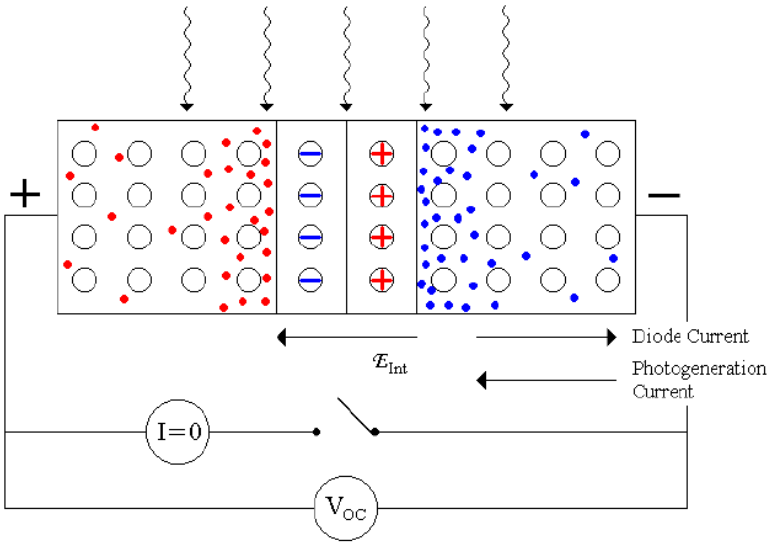

Figure 4. The p-n junction under open circuit conditions V_{OC} (From [2]).

2. Short Circuit Current

Under short circuit conditions, I_{Ph} is able to operate at a maximum since there is no opposing diode current. The I_{Ph} is proportional to the intensity of the sunlight that is creating minority carriers from the EHPs. The I_{SC} is at a theoretical maximum when the cell is subjected to an ideal solar intensity that only exists on the outside boundary of the earth's atmosphere. However, since solar cells are predominantly used in less than ideal environments, a practical I_{SC} maximum is achieved during direct sunlight conditions. Figure 5 is a depiction of a solar cell during short circuit conditions.

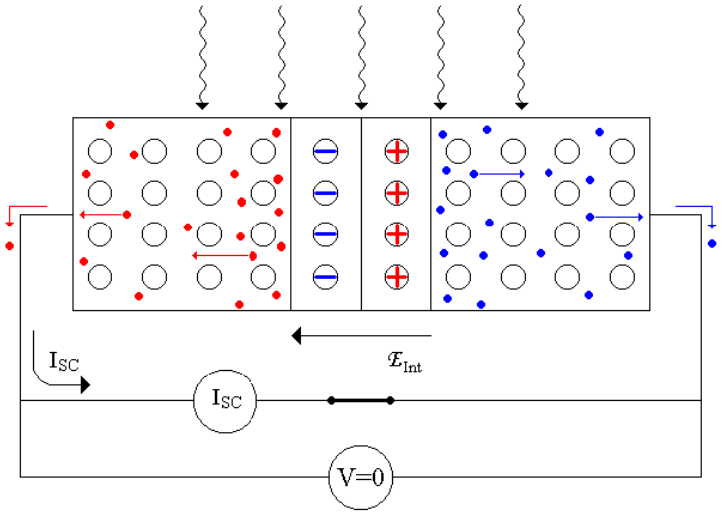

Figure 5. The p-n junction under short circuit current conditions (From [2]).

The total current I of a solar cell is defined as the diode current minus I_{Ph} and is described by

$$I = I_0(e^{qv/kT}) - I_{Ph} \,. \tag{2-6}$$

3. Efficiency and Fill Factor

The maximum output power P_{out} of a solar cell related to the input power P_{in} that is generated by the photons incident on a cell is a measure of its efficiency and is described by

$$\eta = \frac{P_{out}}{P_{in}} \,. \tag{2-7}$$

As described by

$$FF = \frac{I_M V_M}{I_{SC} V_{OC}} \,, \tag{2-8}$$

the FF is a measure of the quality of the solar cell and is the ratio of the product of the maximum voltage V_M and current I_M operating points that yield the maximum amount of power to the product of V_{OC} and I_{SC}. Figure 6 is a depiction of a current-voltage (I-V) curve for a solar cell. The closer the I-V curve approaches the shape of a rectangle, the higher the fill factor. Typical FFs for high quality cells range from 0.75 to 0.85.

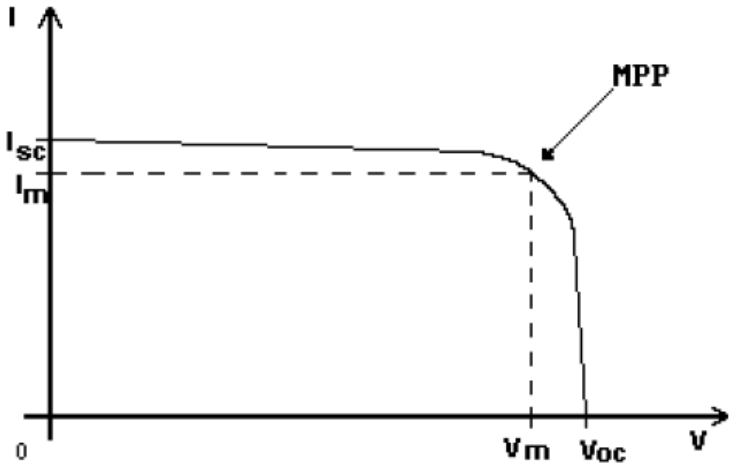

Figure 6. A typical I-V curve with MPP depicted (From [2]).

C. SOLAR CELL EFFICIENCY VARIABLES

A majority of the energy obtained from sunlight is exhausted prior to ever reaching a PV cell by both internal and external factors. These factors directly affect the efficiency of the solar cell by governing how much solar energy is actually converted into electrical energy.

1. Irradiance

Irradiance is defined as the amount of solar radiation received per unit area on a particular surface [4]. Irradiance varies based the seasonal location of the earth with respect to the sun, the position of sun in the sky throughout a given day, and the weather [5]. The irradiance of the sun at the boundary of our atmosphere is approximately 1.360 kW/m^2 and is referred to as the solar constant, or air mass zero (AM0) [6]. The standard spectrum of sunlight available at the earth's surface in the equatorial and tropical regions when the sun is directly overhead is described as air mass one (AM1). Due to a majority of the world's population living at higher latitudes than the equator and atmospheric attenuation variables, the solar industry has agreed upon a standard solar intensity of 1000 kW/m^2, or AM1.5, to classify and test solar panels [7].

2. Recombination

Direct and indirect internal recombination is the elimination of charge carriers, both electrons and electron holes, which occurs at the surface of the semiconductor, in the bulk of the solar cell, and to a lesser extent, in the depletion region. When recombination occurs at the surface of the semiconductor, energy may be transferred into the band gap causing electrons to fall back into the valence band and recombine with holes. The effects of recombination at the semiconductor surface can be mitigated by using purer semiconductor materials. The other primary source of electron-hole recombination occurs in the bulk of the

substrate and is caused by Auger recombination, Shockley-Read-Hall recombination, and radiative recombination [7].

3. Temperature

Low energy photons (i.e., less than 1.1 electron volt for silicon) will create heat that may lower cell efficiency. Additionally, photons with too much energy will create an EHP but will also increase cell temperature. Lattice vibrations due to high or low temperatures interfere with the flow of charges and results in non-optimal operation. For silicon cells, there is an approximate 2.3 mV per cell decrease in open-circuit voltage when the temperature raises one Celsius [7]. In an average solar cell, only 45% of incident photons are converted to electrical energy. The remaining is dissipated in the form of heat or pass through the material completely [7].

4. Reflection

Reflection of light off the cell surface can be as high as 36% for an untreated surface. The reflection percentage can be reduced to around five percent through the use of antireflection coatings (i.e., silicone oxide) and surface texturing [7].

5. Electrical Resistance

There is resistance to charge and current flow in the bulk of the case, in the surface, and at the contact junction. Additionally, there is ohmic resistance in the metal contacts that provide access to the p-n junction [7].

6. Material Defects and Self-shading

Dangling bonds from impurities and nonperfect crystal structure causes recombination problems. Self-shading from the top electric conductors causes photon reflection off the top electrical grid and can result in losses up to eight percent [7].

THIS PAGE INTENTIONALLY LEFT BLANK

III. MAXIMUM POWER POINT TRAEQUATION CHAPTER (NEXT) SECTION 1CKERS

A. MPPT DESIGN PRINCIPLES

The wide-spread adoption of the utilization of solar energy as a renewable resource is severely limited by the relatively low conversion efficiency from solar to electrical power. A general guideline for most PV systems corresponds to an overall efficiency of less than 17% and is significantly less under low irradiation conditions [8]. This low conversion attribute requires an almost disproportionate quantity of solar cells to generate a modest amount of useful electrical power. Therefore, any device, technique, or advance in technology that increases the energy conversion efficiency of a PV system by even a small amount has a large impact in reducing the quantity of cells and the physical size of the array. Other benefits of optimizing the conversion efficiency include a significant reduction in cost or a substantial increase in the power available to the user.

A common method of maximizing the efficiency of a PV system is the detection and tracking of an array's MPP under varying conditions. The MPP is not constant or easily known; this is due to the nonlinear relationship between a cell's output and input variables (i.e., solar irradiation and temperature) which results in a unique operating point along the I-V curve where maximum power is delivered [9]. When a PV array is connected directly to the load, referred to as a directly-coupled system, the overall operating

voltage of the system is determined by the intersection of the load line and I-V curve as shown in Figure 7 [10].

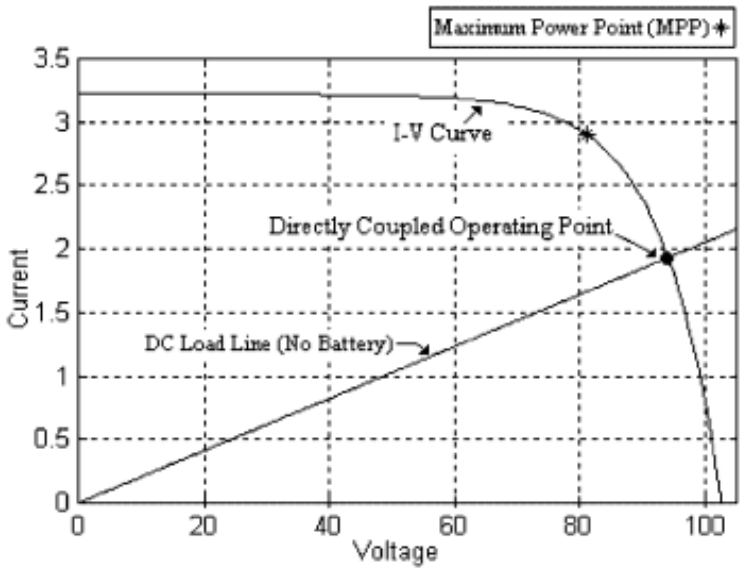

Figure 7. The operating point of a directly-coupled PV array and load (From [10]).

A fluctuating level of irradiance is one of the many nonlinear variables that influence the I-V curve of a PV array. As shown in Figure 8, the intersection of the load line and varying I-V curves due to fluctuating irradiance levels significantly impacts the operating voltage and power output available to the load. The typical solution to account for this nonlinear relationship is to oversize the PV array to ensure the load's power requirements are always met.

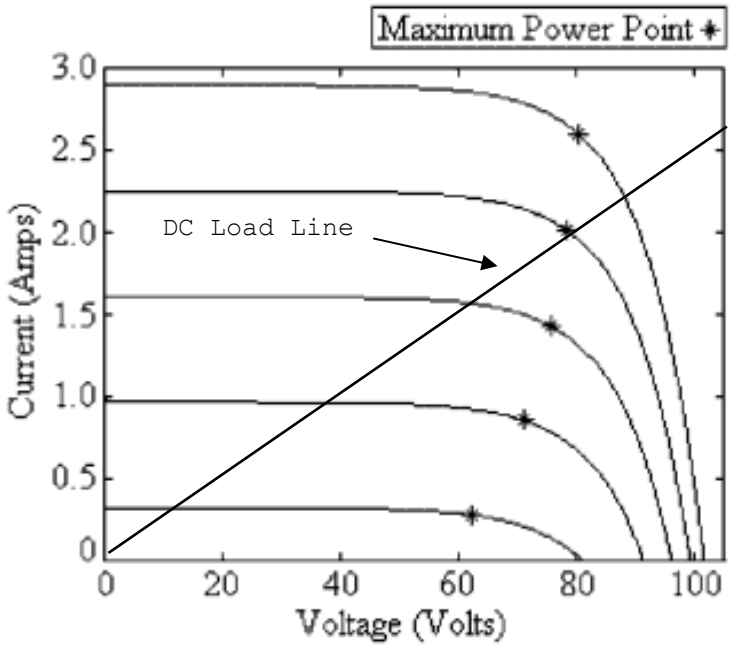

Figure 8. A PV I-V curve at 40°C for different irradiance levels (After [10]).

Although the cost per watt of solar energy has dropped considerably, oversizing an array to account for the worst case I-V curve is cost prohibitive for most applications. An MPPT specifically addresses this scenario and provides a cost effective solution. Simply put, an MPPT is a switch-mode power converter that decouples the array from the load to independently control the array's voltage and current [10]. A modern MPPT uses a micro-controller or analog methods to locate the MPP by using calculation models or more commonly, search algorithms. The proper names of these methods include perturb and observe, incremental conductance, fractional short circuit, fractional open circuit voltage, fuzzy logic, neural networks, pilot cells, and digital signal processor based implementations. Each of these tracking algorithms has been written about

extensively in the literature with varying levels of effectiveness [8]. The more commonly used designs found in commercial applications are summarized in this chapter.

B. ANALYSIS OF TRACKING ALGORITHMS

1. Perturb and Observe

The most common MPPT algorithm utilized is the perturb and observe (P&O); this is due to its simplicity and ease of implementation [10]. The basic premise behind P&O is the algorithm's constant comparison of the array's output power after a small, deliberate perturbation in the array's operating voltage is applied. If the output power is increased after the perturbation, then the array's operating point is now closer to the MPP, and the algorithm continues to "climb the hill" towards the MPP. If the power is decreased, then the operating point is further from the MPP, and the algorithm reverses the algebraic sign of the perturbation in order to "climb the hill." To better illustrate this point, a family of power curves as a function of voltage (P-V curves) at different irradiance levels G is shown in Figure 9. The other major solar input variable, temperature, is held constant. If an array is operating at point A as shown in Figure 9, the P&O algorithm incrementally increases the array's operating voltage until the MPP is reached at the global maxima (i.e., G = 1000 W/m^2).

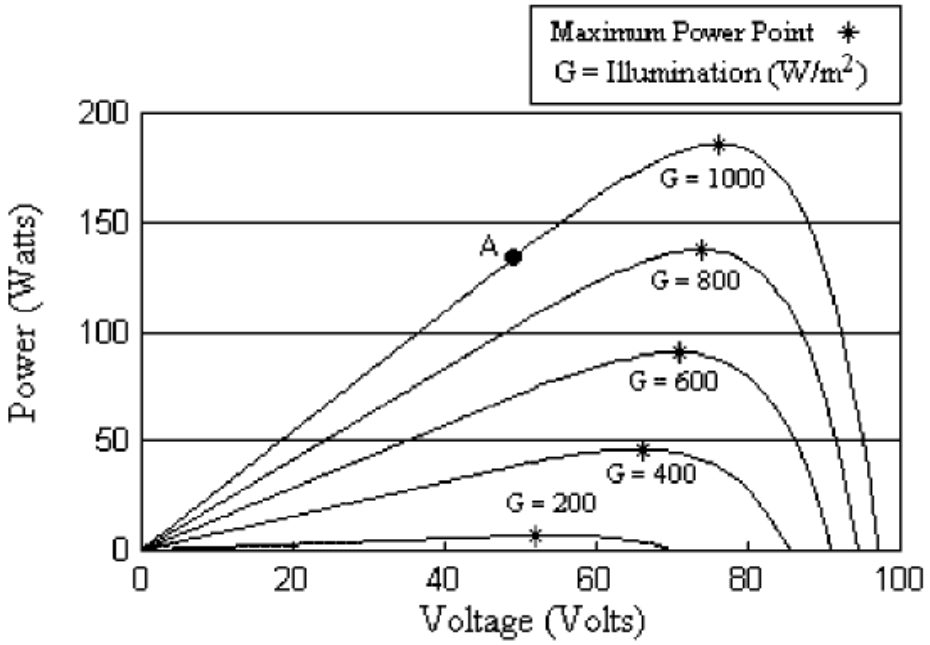

Figure 9. The P-V relationship at different irradiance levels (From [10]).

Despite the simplicity of P&O, there are limitations to its effectiveness [10]. One disadvantage is once the MPP is reached, the P&O algorithm continues to oscillate on each side of the global maxima by changing the sign of the perturbation after each power measurement. This constant searching results in a slight loss in power due to the MPP not settling at the true maxima. Another drawback is a decrease in sunlight causes the P-V curve to flatten similar to the G = 200 W/m^2 curve shown in Figure 9. This causes the change in power after each perturbation to become negligible and makes it difficult for P&O to find the MPP. The P&O algorithm also does not perform well in rapidly changing irradiance conditions since it assumes any change in power is due to its perturbation and not changing environmental conditions. How the P&O algorithm could theoretically be moving away from the MPP (i.e., point A)

during rapidly increasing irradiance levels is shown in Figure 10. This error can quickly be compounded if the system does not spend enough time at a relatively uniform irradiance level to correct the error. Finally and most significantly, P&O's main disadvantage is that the small, incremental perturbations cannot keep up with rapidly changing atmospheric conditions that may cause the MPP to shift by a large amount. This measured approach in finding the MPP results in a considerable amount of lost power [11].

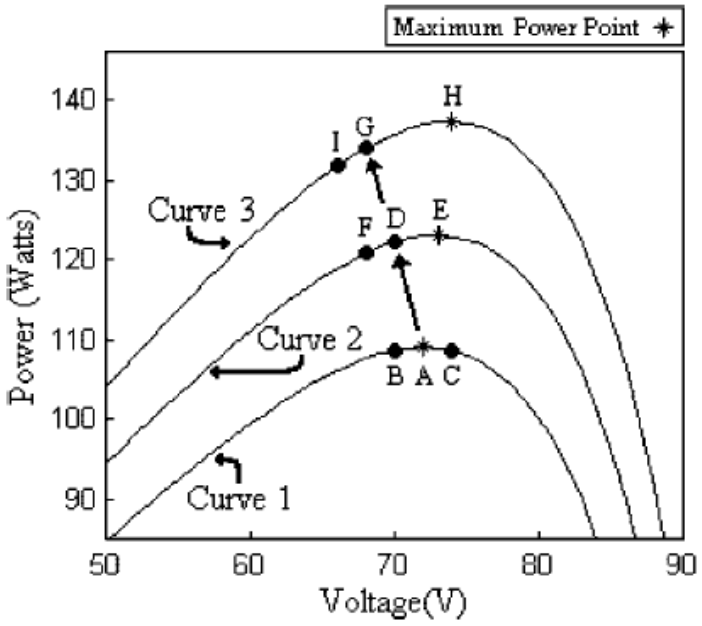

Figure 10. An illustration of erratic behavior when the P&O algorithm is exposed to rapidly increasing irradiance (From [10]).

Several improvements have been proposed to the P&O algorithm to improve its performance. A common modification that provides for a reduction in the number of oscillations that occur in the vicinity of the MPP during constant irradiance conditions is to implement a "waiting" function.

A waiting function identifies when the algebraic sign of the perturbation is reversed multiple times in a row. If this condition is satisfied, the controller assumes it is at the MPP and delays the perturbation process for a defined period of time. This improves the efficiency of the P&O controller during constant irradiance but also makes it slow to respond when conditions do change [10]. Another improvement takes two measurements that compare the array's power at a defined operating point separated by a time interval; any change in the power indicates a fluctuating level of irradiance and can be accounted for during the perturbation process. However, these additional measurements add complexity to the algorithm and make the controller less responsive [10]. In summary, the operating environment of the PV panel must be evaluated before any modification to the original P&O algorithm is considered. Each modification brings specific advantages that may or may not offset any degradation to the overall system efficiency.

2. Constant Voltage and Constant Current

The constant voltage (CV) algorithm is based on the general observation that an array's voltage at the maximum power point V_{MPP} compared to its open circuit voltage V_{OC} can be approximated based upon

$$\frac{V_{MPP}}{V_{OC}} \cong K < 1 \qquad (3\text{-}1)$$

where K is the predetermined value for the ratio [10]. The flow chart in Figure 11 depicts the constant voltage algorithm. In order to measure the open circuit voltage, the solar array is temporarily isolated from the MPPT.

Given Equation (3-1) and the predetermined value *K*, the MPPT adjusts the array's voltage until V_{MPP} is obtained. This simple method is repeated periodically in order to recalculate the V_{MPP} and ensures the solar panel is operating near its MPP.

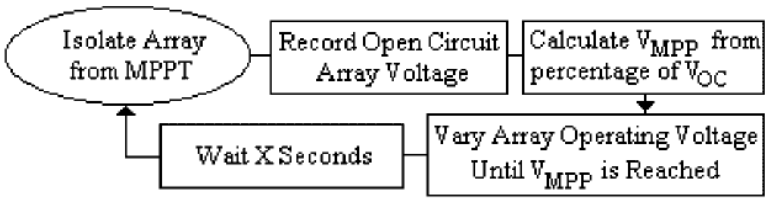

Figure 11. A flowchart depicting the constant voltage algorithm (From [10]).

Literature recommends that the value for *K* should range from 0.73 to 0.80. However, if the panel is exposed to a range of temperatures (i.e., 0 to 60 C) and subjected to varying irradiance levels (i.e., 200 to 1000 W/m^2), it becomes apparent that these variables affect the location of the MPP, and the fixed ratio *K* is unable to adjust the array's V_{MPP}. It can be seen in Figure 12 that *K*, depicted on the y-axis, is dependent on environmental conditions. Since *K* is a fixed, predetermined value, the error can reach as high as eight percent in response to the irradiance and temperature fluctuating [10].

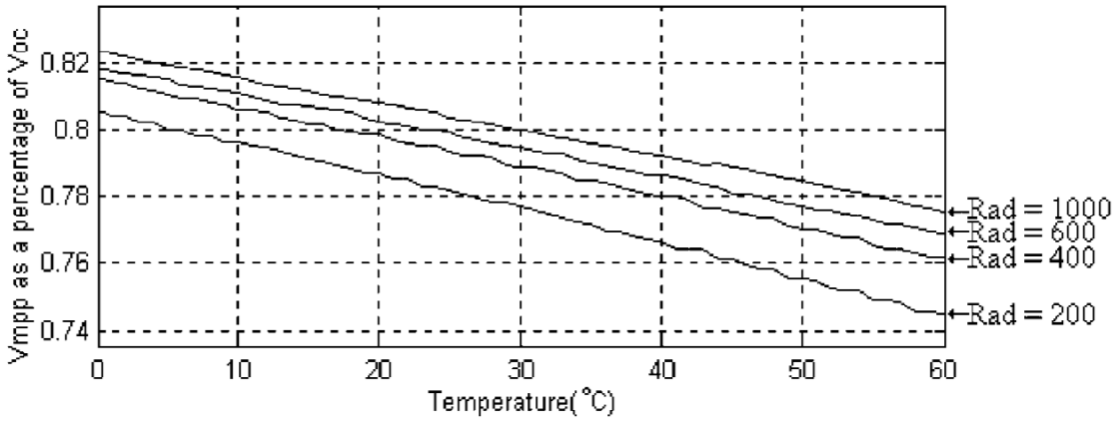

Figure 12. V_{MPP} as a percentage of V_{OC} (constant ***K***) as functions of temperature and irradiance (From [10]).

The main advantages of implementing a constant voltage MPPT is its simplicity and use of relatively inexpensive analog components. However, the MPPT tracking efficiency suffers when compared to other algorithms. Specific reasons include the error associated with selecting a constant ratio ***K*** and that the panel's output power is temporarily interrupted each time the V_{OC} is measured. A search algorithm could be added to dynamically adjust the value of ***K*** to account for the changing environmental conditions, but this is typically not done since the final design ends up being very similar to P&O [10].

A constant current algorithm works in a similar manner by approximating the MPP current as a certain percentage of the I_{SC}. To obtain the I_{SC}, a switch is placed across the input terminals of the converter and is momentarily closed. The MPPT then adjusts the array's output current to match the calculated MPP current. Although simple in theory, it is difficult to establish zero resistance across the array's terminals to obtain a true short-circuit current

measurement. Thus, constant voltage MPPTs are preferred due to the relative ease of measuring voltages vice short circuit currents [10].

3. Pilot Cell

A pilot cell MPPT algorithm utilizes a small solar cell called a pilot cell that has the same characteristics as a larger PV array. The constant voltage or current method is applied to the pilot cell in order to obtain the V_{OC} or I_{SC} measurement. The calculated MPP can then be applied to the larger array without the loss of power that occurs during the V_{OC} or I_{SC} measurement. Disadvantages to this method include utilizing a constant K that does not adjust for temperature and irradiance fluctuations. Additionally, the initial cost of the system is increased due to the requirement that the characteristics of the pilot cell must be calibrated to match the larger array [10].

4. Incremental Conductance

The incremental conductance algorithm differentiates the PV array power with respect to the voltage dP/dV and then sets the result equal to zero [10]. If the PV array is at the MPP, then the algorithm can be summarized by

$$\frac{dP}{dV} = \frac{d(VI)}{dV} = I + V\frac{dI}{dV} = 0 \tag{3-2}$$

which can be rearranged to give

$$-\frac{I}{V} = \frac{dI}{dV} \tag{3-3}$$

where dI/dV is the current differentiated with respect to the voltage. It is important to relate Equation (3-3) to the incremental conductance algorithm. The left-hand side of Equation (3-3) represents the array's instantaneous conductance, while the right-hand side represents the incremental conductance [10]. At the MPP, these quantities are equal to zero but contain the opposite sign. As the array operating point moves away from the MPP, the set of equalities given by

$$\frac{dI}{dV} = -\frac{I}{V};\ \left(\frac{dP}{dV} = 0\right) \tag{3-4}$$

$$\frac{dI}{dV} > -\frac{I}{V};\ \left(\frac{dP}{dV} > 0\right) \tag{3-5}$$

$$\frac{dI}{dV} < -\frac{I}{V};\ \left(\frac{dP}{dV} < 0\right) \tag{3-6}$$

can be used to define if the array is above or below the operating point. Note that Equation (3-4) is the same as Equation (3-3) but is repeated to signify the equilibrium point of the algorithm (i.e., the MPP). Equations (3-5) and (3-6) are used to determine the direction of the perturbation to reach the equilibrium point. Once Equation (3-4) is satisfied, the MPPT operates at this point until a change of current is detected that is caused by a change in the irradiance [10]. If $dV = 0$ and $dI = 0$, then no environmental changes have been detected and the MPPT is operating at the MPP. If $dV = 0$ and the irradiance increases, causing $dI > 0$, then the MPP voltage also increases. The MPPT will then increase the array's operating voltage to follow the rising MPP. If the irradiance decreases, then $dI < 0$, and the MPP voltage is

lowered causing the MPPT to decrease the array's operating point. Equations (3-5) and (3-6) are additionally used to determine the direction of the voltage to reach the MPP if the changes in the voltage and current are not zero. For example, if $dI/dV > -I/V$, then $dP/dV > 0$, and the operating point is to the left of the MPP on the power versus voltage curve. This will cause the MPPT to increase the array's operating voltage to reach the MPP. If $dI/dV < -I/V$, then $dP/dV < 0$, and the operating point is now to the right of the MPP on the power versus voltage curve. The MPPT will reduce the array's operating voltage to track the MPP. To summarize, the incremental conductance algorithm can be tedious due to its ability to adjust the array's operating point based on changes in the dV, dI/dV, or dI values. This algorithm is depicted graphically using a flowchart as shown in Figure 13.

The primary advantage of using incremental conductance vice a P&O algorithm is its ability to calculate the direction of the perturbation to reach the MPP and its ability to determine when it actually reaches the MPP. This characteristic is particularly useful during rapidly changing irradiance conditions because incremental conductance, unlike P&O, does not track in the wrong direction and does not oscillate once it has arrived at the MPP [10].

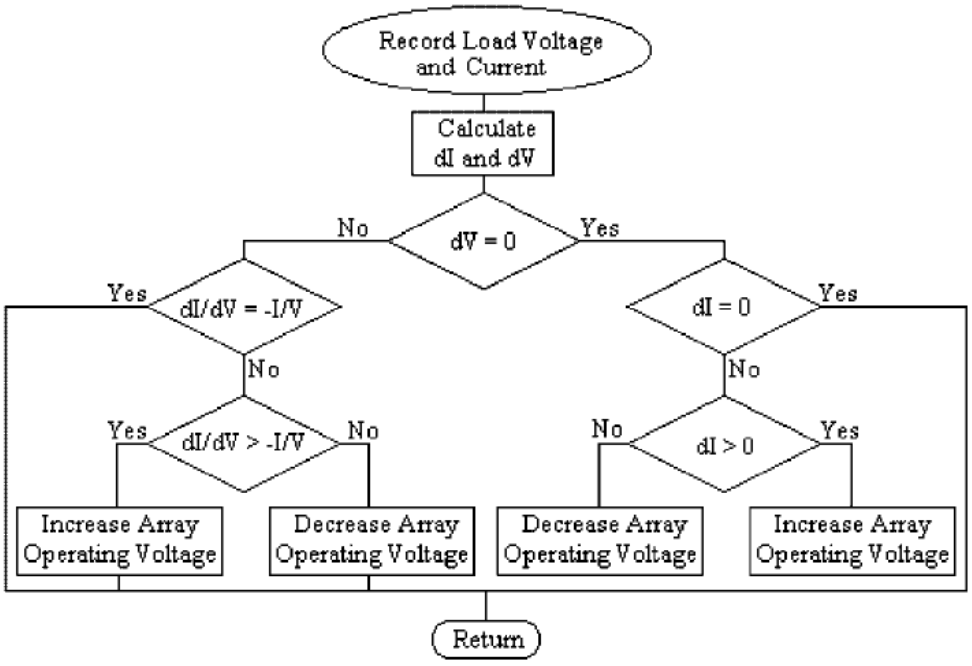

Figure 13. A flowchart of the incremental conductance algorithm (From [10]).

5. Model-based Algorithm

A model-based algorithm can be utilized if the solar cell parameters listed in the equation

$$I = I_L - I_{OS}\left[\exp\frac{q}{Ak_BT}(V + IR) - 1\right] \qquad (3\text{-}7)$$

are known. Equation (3-7) is referred to as the Shockley equation for an illuminated p-n junction where A is the diode ideality factor, q is the charge on an electron, and R is the array's series resistance. Additionally, I_L is the light-generated current as a function of G in W/m^2, and I_{OS} is a function of the reference reverse saturation current. If these values are known, then the solar cell's current and voltage can be calculated by measuring the value of incident light and the temperature of the solar cell. Then

the V_{MPP} can be calculated and set equal to the array's operating voltage. Although this algorithm is relatively simple, its implementation is not realistic due to unknown cell parameters that can change significantly with each production run. Additionally, the light sensor (i.e., pyranometer) required to accurately measure the level of irradiance causes model-based MPPT algorithms to be cost prohibitive [10].

6. Parasitic Capacitance

The parasitic capacitance algorithm uses the illuminated light equation described in (3-7) and adds the charge stored in the p-n junction of the solar cell which is also known as the parasitic junction capacitance C_P. If C_p is represented by $i(t) = CdV/dt$, then (3-7) can be rewritten as

$$I = I_L - I_{OS}\left[\exp\left(\frac{v_P + R_S I}{A}\right) - 1\right] + C_P \frac{dv_P}{dt} = F(v_P) + C_P \frac{dv_P}{dt} \qquad (3\text{-}8)$$

where v_P is voltage in the parasitic capacitance and R_s is the array's resistance. The right side of Equation (3-8) is rewritten to show that the current I can also be expressed as a function of voltage $F(v_P)$ and the current in the parasitic capacitance. This notation yields the incremental conductance of the array g_P as $dF(v_P)/dv_P$ and the instantaneous conductance of the array g_L as $-F(v_P)/v_P$. The MPP is the point at which $dP/dv_P = 0$ is satisfied. Finally, Equation (3-8) is multiplied by the array voltage to obtain the array power, and the result is differentiated to give

$$\frac{dF(V_P)}{dV_P}+C_P\left(\frac{\dot{V}}{V}+\frac{\ddot{V}}{\dot{V}}\right)+\frac{F(V_P)}{V_P}=0 \tag{3-9}$$

which represents the array's power at the MPP. The individual terms in Equation (3-9) represent the instantaneous conductance, the incremental conductance, and the ripple from the parasitic capacitance. Also note that the first and second derivatives of the array voltage encompass the AC ripple components generated by the converter. It is important to note that if C_P is equal to zero, then the equation becomes synonymous with the equation used for the incremental conductance algorithm. Additionally, since C_p is modeled as a capacitor in parallel with the individual cells, adding additional cells in parallel will increase the capacitance as seen by the MPPT. This translates to a significant difference in MPPT efficiency between the parasitic capacitance and incremental conductance algorithms when utilized in high-power solar arrays with many modules [10].

In order to find the array's conductance, a ratio is established between instantaneous array current to the instantaneous array voltage. Although more difficult, the equation

$$g_P=\frac{P_{GP}}{V_O{}^2}=\frac{\frac{1}{2}\sum_{n=1}^{\infty}\left[a_n^i a_n^v+b_n^i b_n^v\right]}{\frac{1}{2}\sum_{n=1}^{\infty}\left[\left(a_n^v\right)^2+\left(b_n^v\right)^2\right]} \tag{3-10}$$

can be used to obtain the array's differential conductance where P_{GP} is the average ripple power, V_O is the magnitude of the voltage ripple, and a_n^i, a_n^v, b_n^i, b_n^v are the coefficients of the Fourier series of the PV array and current ripple

[10]. A circuit configuration as shown in Figure 14 can be used to obtain the output values of P_{GP} and V_O^2, while the inputs to the circuit are the array's current and voltage. The DC component of the array voltage is removed with the high-pass filters, and the two multipliers create the AC V_O^2, or $\tilde{v}_o(t)$, and the AC P_{GP}, or $\tilde{p}_{GP}(t)$, which are subsequently filtered by the low pass filters to yield the DC components of V_O^2 and P_{GP}. From Equation (3-10), the ratio of these two values is defined as the array's conductance. The algorithm then adjusts the array's operating point until the array's conductance and differential conductance is equal.

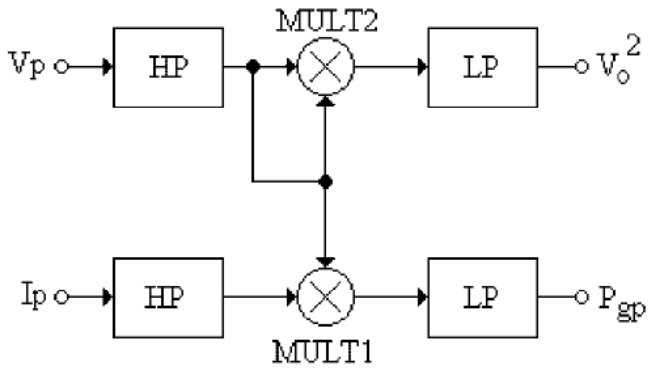

Figure 14. The circuitry used when implementing the parasitic capacitance algorithm (From [10]).

7. MPPT Algorithm Performance

Given the diversity of the various algorithms described thus far, it is difficult to ascertain which method is the best for maximizing an array's output power. Although a certain characteristic of one algorithm might justify its exclusive use, most users of PV arrays are concerned with the efficiency of the integrated system. Therefore, a practical starting point would be to compare

the power output of an MPPT with the actual MPP of an array that is being exposed to a constant temperature and level of irradiance. A comparative study was conducted by [10] in order to calculate the efficiency of a micro-controller based MPPT using the following algorithms: P&O, incremental conductance, and CV. The algorithms were loaded on identical micro-controllers, optimized, and tested on standardized hardware. It can be seen in Table 1 that the efficiency of the P&O and incremental conductance *Inc* algorithms are extremely high. As discussed previously, the CV algorithm is the simplest to implement, but also results in the lowest efficiency.

Table 1. Comparison of MPPT tracking efficiencies (η_{MPPT}) among selected algorithms (From [10]).

Sky conditions	P&O		Inc		CV	
PV array	Days of data	η_{MPPT}	Days of data	η_{MPPT}	Days of data	η_{MPPT}
Clear	20	98·7	17	98·7	20	90·4
Partly cloudy	14	96·5	11	97·0	10	90·1
Cloudy	9	98·1	11	96·7	6	93·1
Overall	43	97·8	39	97·4	36	91·2
Simulator						
Overall	99·3		99·4		93·1	

An updated and more in-depth study compared classical P&O (P&Oa), modified P&O (P&Ob), three point weight comparison P&O (P&Oc), CV, incremental conductance (IC), open circuit voltage (OV), and short-current pulse (SC) [8]. It is important to note that the different variations of P&O all operate in a similar manner to the P&O algorithm described in detail thus far. The minor modification among them is in regards to their perturbation step-size. The step-sizes are either constant (P&Oa), proportional to the

change in power (P&Ob), or averaged among three perturbations (P&Oc). The experiment subjected the different algorithms to changing irradiance levels of either two levels (Case 1) or three levels (Case 2), and the power output was captured once steady-state conditions were reached. As shown in Table 2, the P&Ob algorithm (i.e., a step-size proportional to the change in power) provided the highest amount of energy output in Joules. It is also important to note that classic P&O with a constant step-size, defined as P&Oa, still produced acceptable results [8].

Table 2. A comparative ranking of MPPT algorithms under varying irradiance inputs (From [8]).

MPPT Technique	Case 1			Case 2		
	Energy [J]	Rank	Delta Energy	Energy [J]	Rank	Delta Energy
P&Oa	4282	2	+1,4%	3144	2	+0,8%
P&Ob	4346	1	+0,4%	3212	1	+0,5%
P&Oc	4278	3	+0,4%	3135	3	+1,0%
IC	4215	4	+1,0%	3117	4	+2,7%
CV	4201	5	+2,8%	3100	6	+3,9%
OV	4200	6	+1,3%	3104	5	+2,1%
SC	4088	7	+0,8%	2942	7	-0,9%

C. ANALOG VERSUS DIGITAL MPPT DESIGN

1. Digital Design

Modern power management and renewable energy systems are comprised of multiple subsystems that include power sources, loads, power buses, and converter modules. The use of MPPTs with digital algorithms offers many advantages when interfacing with these subsystems. Digital methods provide for data storage and transmission capabilities that can help system maintenance and debugging. Additionally,

the degradation of components due to age or as a result being exposed to harsh environments can lead to a loss of accuracy for analog controllers [12]. On the complex end of the digital design spectrum, implementing intelligent algorithms such as fuzzy logic and neural networks allow for adaptive control that provides for a responsive controller but results in a cost-prohibitive commercial application due to the additional hardware and computing requirements. In order to realistically integrate digital control into low-cost systems, most digital MPPT controllers utilize a single, closed control loop that manipulates the array input voltage in response to varying environmental conditions. The P&O algorithm is by far the most popular digital option due to its ease of implementation and relatively good performance. Two examples of digital P&O algorithms, classic and adaptive, are compared in this section. However, classic P&O is not explained in detail due to it being discussed at length previously in this chapter. As a summary and a baseline for the new method, classic P&O measures the change in power via a closed control loop that uses a defined step-size to perturb the duty cycle of the controller that results in a small change in the operating point of the array. The primary disadvantages to classic P&O are its slow and possibly incorrect tracking direction when a rapid change in the luminosity occurs [12]. To address the problem of responsiveness, an adaptive P&O control strategy can be implemented to speed up the tracking process. This ability to easily modify microprocessor-based algorithms emphasizes one of the strongest advantages of choosing digital control over analog.

Adaptive P&O modifies the perturbation step-size so that when the difference between the operating point and the MPP is large, the step-size is also large. As the algorithm starts to approach the MPP, it adjusts the step-size to become very small [12]. While this method improves upon the classic P&O approach, the adaptive P&O algorithm can easily be modified to use two, independent control loops to provide even more responsiveness to changing environmental conditions. To better understand the ingenuity of this approach, the concept of dual-control loops will be explored and built upon.

The use of both a power control loop combined with a voltage control loop keeps the adaptive P&O algorithm at a fixed voltage during a rapid change in irradiance. This is illustrated in Figure 15 by comparing the response of a single, power control loop P&O algorithm (point A to B) to the dual-control loop P&O approach (point A to C).

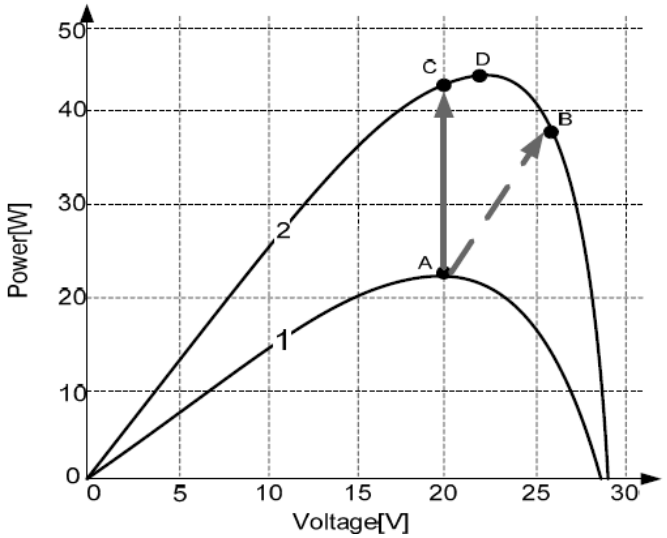

Figure 15. Change of current operating points when the irradiance changes for different adaptive P&O algorithms (From [12]).

By preventing the MPPT from jumping to a greater voltage and current (i.e., point B), the dual-control loop algorithm holds the voltage constant and allows for a change in the current in the same direction that the change in irradiance occurred. The result is that point C is much closer than point B, and the algorithm has less distance to travel to reach the actual MPP (i.e., point D).

To address the problem of possibly tracking in the wrong direction in response to a rapid luminosity change, the dual-control loop P&O strategy can be slightly modified. Instead of monitoring the voltage, the second control loop now tracks the average solar panel input current. In addition to increasing the tracking accuracy of the MPPT, the average current control method produces three other significant advantages:

- The DC-DC converter acts as a current source, and the output is immune to voltage perturbations.
- The current capability of the output can be increased by paralleling multiple converters.
- Short-circuit protection is realized with the current loop [12].

Finally, a novel improvement to this approach combines the average current control method with a variable step-size algorithm that uses a hybrid of the fixed P&O and the three-point P&O methods. As a side note, the three-point method takes the average of three perturbations and adjusts the step-size accordingly. The main advantage to using this hybrid approach is that the complex calculation of computing the slope of the P-V curve is not required in order to determine the magnitude of the step-size. This independence from the dP/dV calculation allows for this

scheme to be used with any solar panel without the requirement to adjust the gain of the current and voltage sensors [12]. Experiments for this novel adaptive P&O algorithm show changes in irradiance resulted in the new MPP being reached in 1.2 seconds [12]. Compared to classic P&O, this adaptive approach provides for a faster transient response time, and the overall time to converge at the MPP is reduced by a factor of two.

The primary conclusion from this section is the performance characteristics of a modern, digital P&O controller that significantly improved upon most of the disadvantages of classic P&O (i.e., response time and tracking error). The 1.2 seconds it takes to reach the MPP represents the best response time of current P&O algorithms and should be used as a general reference during system design.

2. Analog Design

Analog MPPT control strategies are enjoying a reemergence in popularity due to their simplicity, cost effectiveness, and low power requirements. A common strategy when designing an analog MPPT is to utilize a comparator to detect changes in the load current. An analog controller utilizing a load current-based control strategy can be easily integrated into the power converter circuitry as shown in the block diagram of Figure 16. The DC-DC converter regulates the voltage and current of the PV panel and, therefore, controls the output power. The analog MPPT controller continuously adjusts the duty cycle of the power converter to ensure the MPP of each panel/cell is achieved [13]. Although the analog algorithms described in this

section each track the MPP in a different manner, they are all comprised entirely of analog components and are dependent on comparing changes in the load current after an input variable is modified. Two examples of analog control are explained in further detail below and were chosen due to their popularity and ingenuity, respectively.

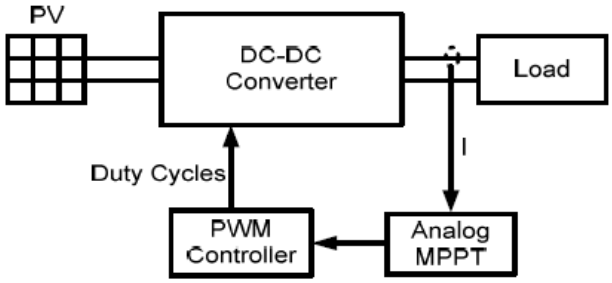

Figure 16. A PV System with a load current-based analog MPPT controller (From [13]).

a. Analog Perturb and Observe of the Load Current

Forced changes in the load current are caused by a P&O control strategy that continuously adjusts the duty cycle of the controller while observing the output current. As long as the output current increases due to the disturbance, the next disturbance should be in the same direction. A simulation of a simple P&O analog controller has successfully demonstrated load current comparison by increasing the load current (i.e., delivering more power to the load) as the PV panel generates more power due to increasing irradiance levels [13]. The simplicity and the relatively few components required to implement a load current based control strategy for an analog MPPT is shown in Figure 17.

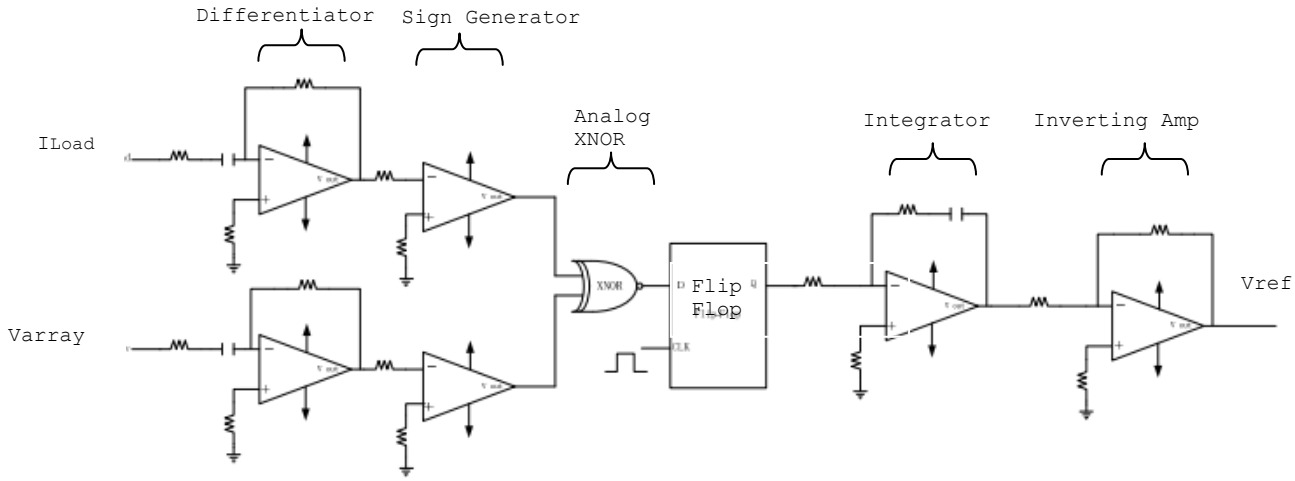

Figure 17. Schematic of a basic analog MPPT controller (After [13]).

The significance of how simple and small this controller can be designed may not be readily apparent; its impact reaches beyond just an improvement in the reliability of the MPPT. By using complementary metal–oxide–semiconductor (CMOS) technology to implement this analog circuit controller with a power converter, the entire MPPT can be fabricated as an integrated circuit unit and can be attached to individual cells within a PV panel. This will lead to a flexible power management architecture that is able achieve per-cell MPP tracking in order to provide a higher amount of output power [13]. Additionally, the entire PV system will achieve agility and resilience and be capable of maximizing power output during challenging environmental conditions such as partial shading or cell degradation/damage.

b. TEODI

Technique based on Equalization of the Output operating points in correspondence of the forced Displacement of the Input operating points of two identical systems (TEODI) is a newer analog MPPT technique that is simpler than digital methods, requires no memory and multiplication operations, and still provides a high level of efficiency when compared to P&O methods. The main advantages of utilizing TEODI to detect the MPP are the following [14]:

- Implementation is simple and there is no need for a digital microprocessor.
- It does not require a measurement of the PV panel's current and voltage.
- Since the PV panel's power output is not tracked, this leads to a simpler controller design with fewer components. Less components increase reliability.
- It can be used with any type of power converter technology.
- A very high efficiency can be achieved since there are no fluctuations at the PV operating point.
- When connecting to the power grid, the 60 Hz disturbances that may cause a failure in the P&O algorithm are avoided when using TEODI.
- TEODI is applicable to distributed MPPT operations.

TEODI was originally designed for applications that utilize two identical PV modules operating under the same levels of irradiance and temperature [14]. The optimal application of TEODI is when a PV module is divided into identical submodules that share a single integrated MPPT

controller. However, although an integrated MPPT controller is used, each submodule has its own DC-DC converter. The TEODI approach forces the submodules to operate at the same output voltage since they are operating in parallel with respect to the load. The basic principle behind TEODI is that since the output voltages are the same and the currents produced by the submodules are also identical due to the irradiance and temperature being uniform for both sub modules, the input power of the two DC-DC converters must also be the same value. This can only occur in two cases:

Case 1) if the input operating voltages of the two submodules are the same value

or

Case 2) if the two sub modules are producing the same power, but the input operating voltages *vA1* and *vB1* are located at opposite sides of the MPP as shown in Figure 18 [14].

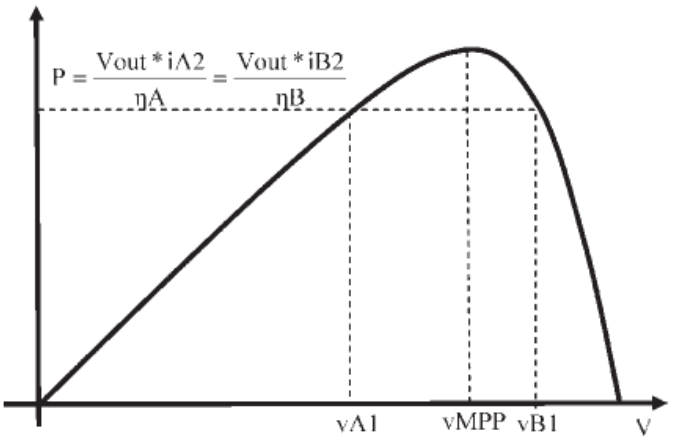

Figure 18. Location of TEODI case 2 operating points on a notional P-V curve (From [13]).

TEODI is able to track and operate at the MPP by ensuring the PV system always operates in the second condition stated above. The TEODI tracking algorithm constantly samples the power output of the submodules and makes adjustments to the input voltage operating points until equalization of the output power is achieved. Although the voltage operating points of the submodules are exaggerated in Figure 18 to illustrate a point, they are in actuality very close to the MPP which results in a high overall system efficiency. Comparing TEODI to an optimized P&O algorithm results in a nearly identical power output at steady state, but it can be shown that a higher tracking speed is achieved using TEODI [14].

In order to achieve the highest efficiency, TEODI requires the differences between the power and voltage characteristics of the submodules to be negligible [14]. The obvious problem with this requirement is that manufacturing identical sub modules that are simultaneously exposed to the same irradiance and temperature is nearly impossible to achieve in practical applications. However, a small modification to the original TEODI design will allow for the algorithm to account for mismatched operating conditions. This is accomplished by the addition of a peak detector that compares the magnitude of the individual output currents and forces the system to operate at the MPP regardless of fluctuating input variables. The addition of a peak detector is inexpensive and requires few analog components; thus, the simplicity and reliability of TEODI is maintained [14].

D. MPPT CONVERTER TECHNOLOGY

The theory behind power conversion is quite varied and can be extremely complex depending on the requirements of the application. The approach required to boost AC voltage in preparation for its journey across hundreds of miles of transmission lines is quite different than the switch-mode inductor converters found in modern, battery-operated electronics. This section purposely avoids a lengthy review of the numerous types of power conversion techniques and the theory behind them. Additionally, although the use of inverters are an important component of large-scale PV systems that directly feed the commercial grid, most users rely on a DC storage element to provide flexibility and control when the PV power is utilized. Therefore, the goal of this section is to focus primarily on inductively fed, switch-mode converters in order to familiarize the reader with the principal DC-DC converter technology used in modern PV system design.

1. Inductively Fed, Switch-mode DC-DC Converters

Inductively fed, switch-mode DC-DC converters are used almost exclusively in portable devices where system size and efficiency are the primary design factors. Size and efficiency also govern the use of multiple MPPTs at the sub-panel level and is instrumental in the ultimate realization of assigning an MPPT to each individual solar cell within a PV system. Although numerous DC-DC converter methods are available, switch-mode converters are primarily discussed due to their almost exclusive use in commercially available MPPTs.

Regardless of whether the input DC voltage is being increased (i.e., boost converter) or decreased (i.e., buck converter), the mechanisms responsible for the energy losses in a switch-mode converter are the same. They include the components responsible for conduction, capacitor-drive, and quiescent power [15]. The primary problem with reducing the physical size of a CMOS based switch-mode converter is the resulting decrease in efficiency. However, advances in finer CMOS technologies that capitalize on shorter minimum channel lengths, higher oxide capacitance, and lower breakdown voltages have resulted in a promising potential for reducing the size of switch-mode converters. For example, a study of CMOS buck converters demonstrated that when varying channel lengths of 0.18 µm, 0.35 µm, and 0.50 µm were optimized, they yielded efficiencies of 93%, 89%, and 79%, respectively. Additionally, this was independent of the converter's operation whether in a continuous conduction mode ***CCM*** or a discontinuous conduction mode ***DCM***. This study concluded that finer pitched technologies yielded higher efficiency as long as leakage current, which often increases with reductions in pitch, does not become a significant portion of the load [15].

This study allows us to assume that improved manufacturing processes will provide a path forward for switch-mode converters to maintain high efficiencies (i.e., greater than 90%) as they shrink. Compared to linear converters, switch-mode converters also maintain a relatively high efficiency when a large voltage differential exists between the input and output. However, as shown by the efficiency curve in Figure 19, this

characteristic does not apply to operating the converter at low or high loads [16]. While industry has created a "soft switching" technique to improve the performance at low loads (i.e., a standby or sleep state), the PV system designer is mostly concerned with maximizing the power from a solar array. Therefore, MPPT applications require a switch-mode converter that is rated at a higher current capacity than necessary to avoid the decrease in efficiency when the converter is heavily loaded. Due to the inductor being the most expensive, largest, and heaviest component of an inductively fed, switch-mode converter, this creates a design tradeoff of gaining improvements in efficiency at the expense of cost, weight, and size.

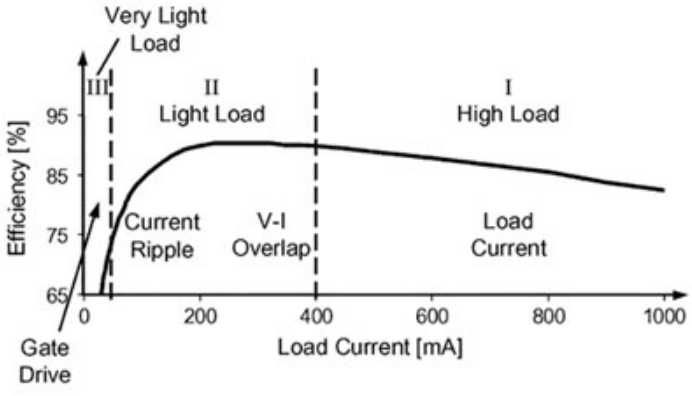

Figure 19. A typical efficiency curve of an inductively fed, switch-mode DC/DC converter (From [16]).

As a possible solution to problem, recent research indicates that integrated, capacitively fed switch-mode converter can achieve respectable performance compared to an inductively fed switch-mode converter of similar capability. This capacitive switch-mode converter operates very similarly and is able to offer both high efficiency and high power density while avoiding the use of thick

metals and magnetic materials that an inductively fed converter must rely on. Due to the savings in weight and size, these advances in capacitor-based converters are of particular interest to integrating MPPTs at the individual solar cell level. The study concluded that capacitor converters had a "bright future" for high power density integrated DC-DC converters [17].

2. MPPT Converter Design

For purposes of PV system design, it is important to gain a perspective on the size of current converter technology. A 300 watt digital P&O MPPT with an inductively fed, switch-mode boost converter is shown in Figure 20. The reader should note that:

- This is a demonstration board provided by the manufacturer and could be shrunk considerably if produced commercially.
- It is capable of 300 watts where per cell applications of MPPTs would only require a few watts.
- As discussed previously, overall MPPT size is primarily determined by the switch-mode converter. This is validated by finding the inductors labeled L1-L4, which also happen to be the largest components on the board.

Using the size of this MPPT and its intended use for larger-scale PV system applications as a reference, we see that it is well within reason to assume that foreseeable advances in DC-DC converter technology will allow for the assignment of an MPPT to each individual cell without significantly impeding the surface area of the array. An ideal example of this per cell application would be if a simple analog MPPT controller and converter was placed directly the beneath solar cell and the electrical

connections were accomplished by vertical interconnect accesses. The resulting increase in cell thickness would be slight, and the PV system's resiliency and performance would be significantly improved. The feasibility of this per cell concept is heavily dependent on the assumption that switch-mode converters will likely continue to shrink without sacrificing efficiency.

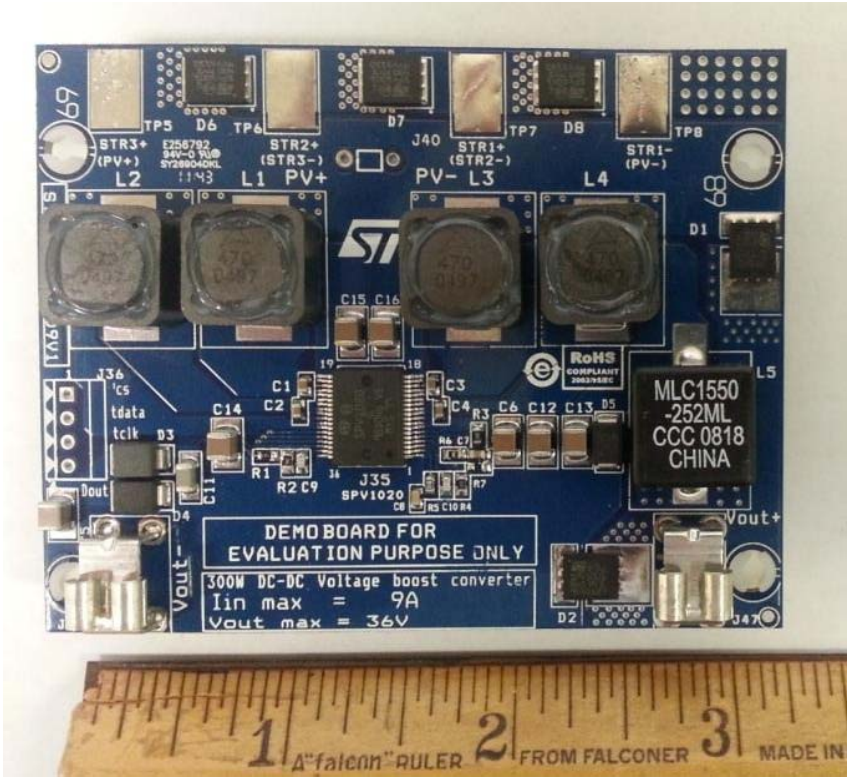

Figure 20. The size of an evaluation board containing a 300 watt digital MPPT with boost DC-DC converter.

IV. POTENTIAL APPLICATIONS

A. INTRODUCTION

The primary advantage of coupling an MPPT with a PV array is to ensure the maximum energy is captured despite the changing of input conditions or output requirements. Consider the example of a PV panel comprised of a series of 60 cells that produce approximately 30 volts DC under a no-load condition (V_{OC} = 30 V). The PV array is then coupled directly to a 24 V battery, and the entire system operates at a load voltage of 24 V. This arrangement is referred to as direct loading, and its primary shortcoming is the low probability that the system's operating voltage is the exact same voltage necessary for the array to be operating at its V_{MPP}. Additionally, even if an array was purchased that had a V_{MPP} of approximately 24 V, the MPP is a shifting target that is dependent on a host of nonlinear input variables such as irradiance, temperature, and cell degradation.

Another disadvantage of directly connecting your PV panel to your battery is the almost certain consequence of overcharging. Overcharging will quickly ruin a lead-acid battery and can cause a fire or explosion when using lithium-ion batteries. Therefore, when designing a PV system, another critical device called a solar charge controller is required to be placed in-between the PV panel and the battery. Charge controllers are designed to charge different types of batteries with a specific voltage and

current profile that prevents damage and improves the performance of the energy storage system.

The three components described thus far are simple, relatively inexpensive, and reliable. It is no surprise that they comprise a majority of the PV systems in use today. Unfortunately, these same PV arrays either fail to operate at their maximum potential or as a deliberate work-around, the arrays are oversized in order to guarantee a certain amount of power is delivered to the load. However, oversizing an array is an expensive solution when using high quality solar cells or may be impossible with respect to applications that have limited surface area (i.e., satellites). Thus, when designing a more sophisticated PV system, the motivation for using an MPPT reaches beyond just the extra power that is gained when the array is forced to operate at its true potential. A relatively inexpensive MPPT can save thousands of dollars when large arrays are built or can make the difference between a sensor being included on a satellite or not. Modern MPPTs are small, efficient, and are becoming so inexpensive the PV industry is not just using one MPPT per array but assigning an MPPT to each sub-panel within an array.

B. A CASE FOR MULTIPLE MPPTS

Consider the 30 V DC panel mentioned previously is now connected in series to other panels to effectively create a single array capable of producing an output rating of 300 V DC. This array is connected to an MPPT, and its output is run through an inverter which converts it to standard AC voltage for household use. Arranging the PV system in this

linear manner is referred to as a central (or standard) inverter design. Its main problem is that the degradation of a single panel has a disproportionate effect on the performance of the entire array. For example, if one panel has a three percent higher resistance as a result of a manufacturing deformity, the entire array performs three percent worse [18]. A multitude of other factors that occur at the individual panel level can also disproportionately reduce the output of the entire string. For example, shading, debris, and snow are common environmental factors that typically only affect a portion of the array as shown in Figure 21. The use of a single MPPT at the array output cannot account for this localized degradation. The problem being that if a solar panel operates at a different point for whatever reason, the MPPT can only see how the entire array was affected and adjusts its operating point based on the change. In certain circumstances, shading just 10% of one portion of the array can reduce the entire PV system power output by as much as 50% [19].

Figure 1. An example of a severely obstructed panel. Note the four panels completely unobstructed (From [18]).

One solution to the panel degradation problem described above is to assign an individual MPPT with an inverter to each 30 V panel. The modified PV system now consists of ten unique arrays connected in parallel that independently track each panel’s MPP while still inverting the output to standard household AC voltages. Manufacturers who are attempting to capitalize on this distributed MPPT concept refer to them as micro-inverters and claim between 5–25% improvements in the output compared to the central inverter method. While the upper end of the range may be overstated, most established micro-inverter companies are advertising improvements between 5–8% [20].

The above example focused on micro-inverters due to the assumption that the reader is familiar with the requirement to convert renewable solar energy into AC power for household use. However, the distributed MPPT architecture described thus far is equally applicable to DC applications (i.e., micro-converters), and the improvements to the output power are similar. This per-panel application of MPPTs is quickly becoming a standard in the PV industry due to a multitude of economic and engineering variables favorably aligning with the increased interest in solar renewable energy. Specifically, the improvements in converter efficiency and their rapidly shrinking size and cost have allowed the micro-inverter approach to be price competitive. In 2010, the price of using micro-inverters averaged 52 cents per watt where the central inverter design was approximately 40 cents per watt [21].

Although a higher price per watt is a significant disadvantage to the micro-inverter approach, additional benefits may make up the difference. They include:

- Higher reliability–Since micro-inverters are not subjected to as high power and heat loads, they last longer. Manufacturers typically offer warranties of 20–25 years for micro inverters and 10–15 years for central inverters.
- Flexibility in future requirements–Expansion of the micro-inverter system is cost effective since each panel operates independently. Central inverters would require a second large inverter to be installed and possibly the rewiring of the existing panels.
- Distributed approach–Micro-inverters prevent localized disruptions from affecting the entire system. If something is wrong with a solar panel or the corresponding micro-inverter, the rest of the system is unaffected.
- Safety–Central inverters typically require higher voltage wiring to handle the 300–600 V DC voltage potential that results from connecting panels in series. Micro-inverters improve safety by eliminating the need for high voltage wiring since each panel is inverted and directly tied to the AC grid.
- Noise–Central inverters may require active cooling (i.e., fans) to dissipate large amounts of heat. Micro-inverters utilize passive-cooling.

Despite these numerous benefits, some applications still do not justify the added expense. For example, consider the case of a homogeneous PV system (i.e., similar panels) that is equally subjected to the same input conditions as shown in Figure 22. Although minor degradations would still be present between each panel, most of the system would operate at a similar MPP. While some advantages of the micro-inverter method are still

relevant, the resulting power output between the two approaches would be very similar, making the decision to use a central or micro-inverter approach much less straightforward.

Figure 2. An example of a homogeneous array exposed to similar environmental conditions.

Keeping this example in mind, generalized recommendations about the use of micro-inverters can be made to the PV system designer. First, micro-inverters excel when portions of the array are being subjected to a dynamic range of input conditions. Second, micro-inverters should be used when a degree of resiliency is desired in the system. In other words, by operating independently, degradation or failure of one panel does not disproportionately affect the performance of the entire array. Finally, micro-inverters should be used when system longevity is a primary concern or when access to the array is difficult. Micro-inverters typically outlast large central inverters and can extend the service life of specialized applications such as satellite systems. The

examples outlined in the remaining sections of this chapter are hypothetical scenarios that the author suggests could benefit from the use of multiple MPPTs.

C. SPACE APPLICATIONS

The Petite Amateur Navy Satellite PANSAT was a "tumbler" satellite designed and built at the Navy Postgraduate School with the aim of providing a small, low-cost, spread spectrum communication satellite for message relay. The satellite was launched by the space shuttle in 1988, and an image of the satellite is shown in Figure 23. Its power system specifications include:

- 17 panels available (total area of 1209 cm^2).
- Each panel has 32 silicon cells connected in series for primary power. A minimum efficiency of 14.5% at AM0 and 28C is required.
- Nickel-cadmium batteries for eclipse power.
- 12 V DC bus voltage.
- 10 W end-of-life power requirement.

Figure 3. An image of PANSAT (From [22]).

Although this satellite is in constant rotation once deployed, this example focuses on the power available at a specific moment in time. For the following calculations, the top of the satellite is normal to the sun as depicted in Figure 24. In this orientation, the center panel receives the full irradiance available from the sun, while the four surrounding panels are situated at a 45^0 angle. As a general rule, if a surface is not normal to the sun, the solar irradiance falling on it will be reduced by the cosine of the angle between the surface normal and the incident ray.

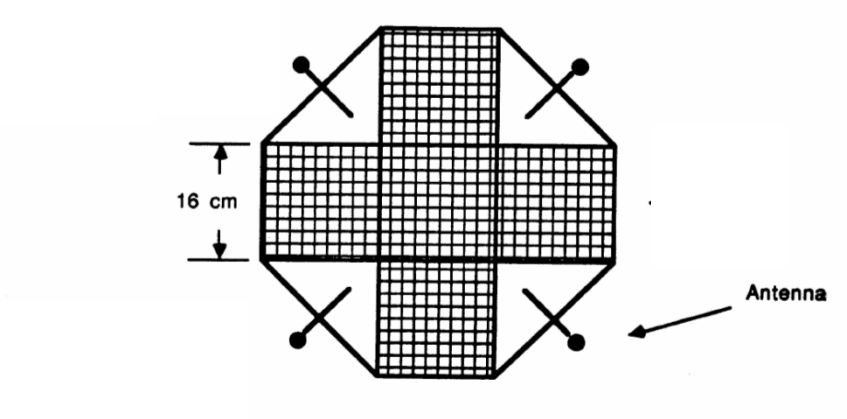

Figure 4. Top view of the PANSAT satellite (From [22]).

1. Direct Loading Versus Central Converter Approach

The performance of the five panels wired together in parallel (i.e., a single array) can be represented by the hypothetical I-V curve shown in Figure 25.

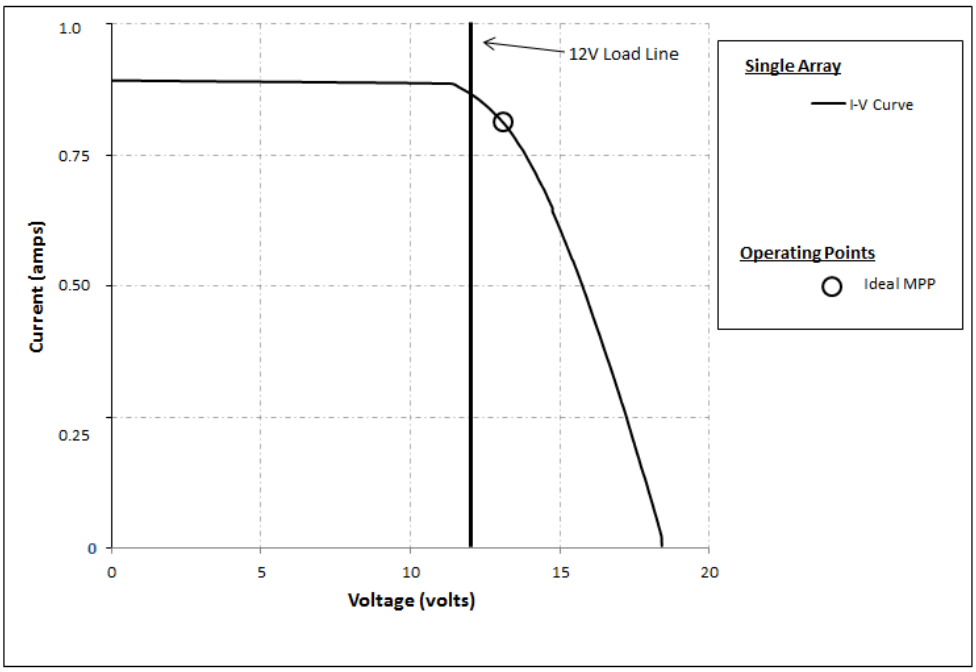

Figure 25. Hypothetical I-V response curve of a PANSAT satellite wired as a single array.

When the single array configuration is subjected to direct loading, the power delivered is approximated by

$$P_{out} = (V_{Load})(I_{Load}) = (12V)(0.86A) = 10.32W \qquad (4-1)$$

where the operating voltage V_{Load} and current I_{Load} are obtained by identifying where the 12 V load line intersects the I-V curve as seen in Figure 25. When the system is configured for use with a single MPPT that has an efficiency of approximately 94%, the power delivered is approximated by

$$P_{out} = \eta_{conv.}\left[(V_{MPP})(I_{MPP})\right] = 0.94\left[(13.2V)(0.80A)\right] = 9.93W \qquad (4-2)$$

where the values are obtained by multiplying the efficiency of the MPPT by the MPP of the array.

Clearly, the use of a single MPPT, or central converter, is not feasible since the minimum end-of-life power requirement of 10 W is not met. While this example is extremely limited in its scope, the designers of PANSAT purposely designed their array to deliver a MPP around the expected 12 V load requirement. When using a single MPPT, the approximate six percent loss that results from the algorithm tracking error and DC-DC conversion process is greater than the minor loss of power that results from operating the array near, but not at, the V_{MPP} under the direct loading method. However, recall that a single MPPT cannot identify localized problems within the array. In most instances, it only takes one moderately degraded panel to disproportionately affect the entire system. In an attempt to lessen the effects of dissimilar irradiance levels, in the next section the use of micro-converters to treat each panel separately in order to outperform the direct loading method is considered.

2. Micro-converter Approach

The effects of treating each panel separately can be represented by the hypothetical I-V curves shown in Figure 26. Note that the solid curved line represents the top panel that is normal to the source, while the dotted curve line represents the four offset panels being exposed to uniformly smaller irradiance levels (i.e., the dotted line is actually four overlapping lines). It can be seen that the MPP of the top panel is 12.7 V which is relatively close to the load voltage of 12 V. However, the four offset panels have a MPP of 14.1 V and are operating 2.1 V below their true potential under the direct loading method.

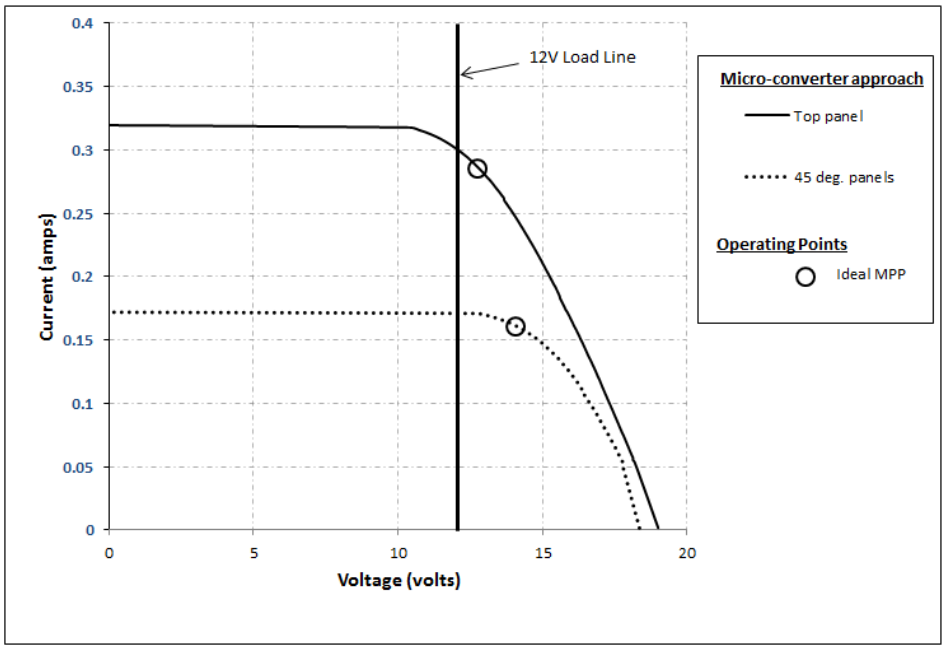

Figure 26. Simulated I-V curve response of a PANSAT satellite using them micro-inverter approach.

When the micro-converter approach is used with MPPTs that have an efficiency of approximately 94%, the power delivered is approximated by

$$P_{out} = \eta_{conv.}\left[(V_{MPP\_top\_panel})(I_{MPP\_top\_panel}) + (4)(V_{MPP\_offset\_panel})(I_{MPP\_offset\_panel})\right]$$

$$P_{out} = 0.94\left[(12.7V)(0.28A) + (4)(14.1V)(0.16A)\right] = 11.83W \quad (4-3)$$

where the values are obtained by multiplying the efficiency of the MPPTs by the MPP of each independent panel. The P-V relationship of the micro-converter approach is shown in Figure 27. It can be seen that the four panels that are offset by 45° have a significantly different MPP than the top panel. Although only 94% efficient, the micro-converter approach surpassed the direct loading method by 1.51 W, or 15%.

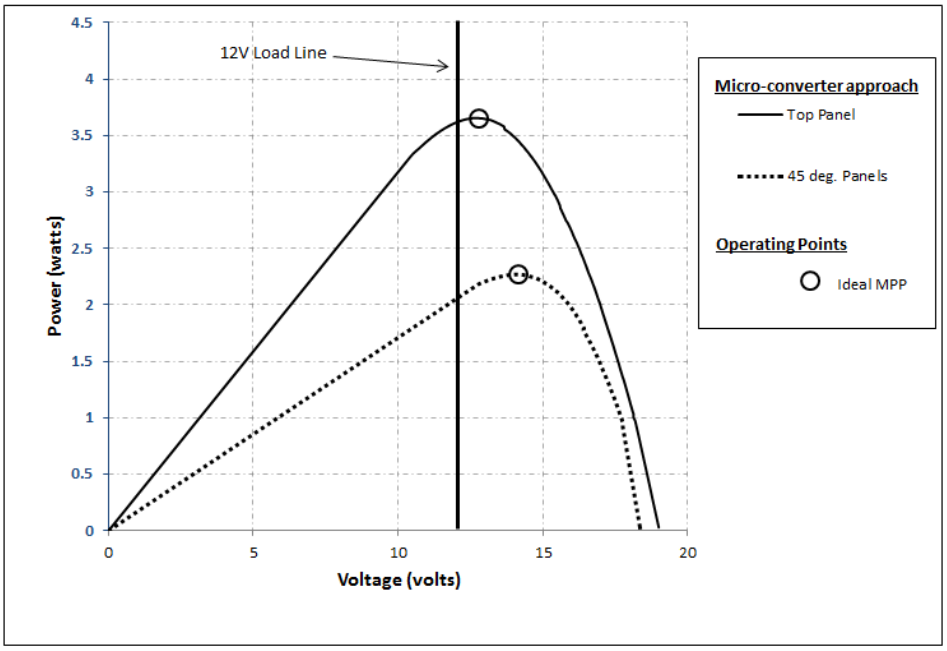

Figure 27. Simulated P-V curve response of a PANSAT satellite using the micro-converter approach.

The purpose of this example was to provide a practical demonstration of using the multiple MPPT approach. The PANSAT satellite is an ideal illustration of individual panels being exposed to drastically different input conditions. However, for simplicity's sake, this example infers the use of certain ideal characteristics of MPPTs and ignores the rotating aspect of PANSAT. When designing with MPPTs, each tracking algorithm and conversion method has its disadvantages that may render the use of MPPTs impractical. Applying this logic to PANSAT, we see that using a P&O MPPT that has a relatively slow tracking algorithm may not be beneficial if the rotating "tumbler" satellite exceeds the MPPT's tracking capabilities. However, innovations and decreasing prices in the solar

industry is enabling a revolution in the type of applications suitable for solar cells. No longer is the use of solar cells reserved for highly specialized applications where solar power is the only practical long-term energy solution. As outlined in the next section, solar cells are currently being used in applications that just a few years ago would have been impossible due to the cost and weight of traditional silicone cells. Thus, it is expected that the traditional use of MPPTs will also evolve and their strengths and weaknesses must be considered to ensure desired performance is met.

D. MILITARY APPLICATIONS

Two current examples of military applications where using multiple MPPTs may be beneficial are presented in this section. Recall, the multiple MPPT design principles suggested in Chapter III are still applicable. Specifically, the micro-converter approach excels when portions of the array are subjected to significantly different input conditions and/or when a high degree of system resiliency is desired.

1. Tactical Solar Tents and Shelters

Until recently, traditional solar panels were comprised of crystalline silicone cells that are housed in a metal frame and protected with a glass cover. These traditional solar panels were rigid, expensive, and heavy. However, recent advances in amorphous silicon cells, otherwise known as thin film technology, has increased the efficiency of flexible cells from approximately six percent to 14% [23]. This large increase in efficiency has provided

for the development of numerous thin-cell applications that meet the military's requirements for ruggedness and power output. For example, the Tactical Solar Tent from Energy Technologies, Incorporated, shown in Figure 28, can provide up to 190 watts of solar power for each 8' x 9' shelter section. However, similar to the 45° offset panels on PANSAT, the solar panels on the tent that are not normal to the sun disproportionately reduce the performance of the entire PV system. It is safe to assume that real-world applications of tactical solar blankets and tents will result in non-ideal PV array configurations such as depicted in Figure 28. Additionally, tactical applications are especially vulnerable to localized disruptions such as shading or cell damage due to the dynamic environment they will be operating in. The micro-converter approach would be beneficial by allowing each panel to operate at its MPP while providing a greater degree of reliability and durability.

Figure 28. The Energy Technologies, Inc. Tactical Solar Tent (From [23]).

2. Unmanned Aerial Vehicles

The same advances in thin film solar cells that have made tactical solar blankets and tents practical can also be used in other military applications. For example, the military and other government agencies have bought tens of thousands of unmanned aerial vehicles *UAVs* of varying sizes in the past ten years. A significant disadvantage to UAVs, particularly smaller platforms, is their short flight time due to a lack of a lightweight, high-capacity energy source. The AeroVironment Raven RQ-11 platform shown in Figure 29 is an example of a smaller UAV that has approximately 60–90 minutes of flight endurance before its batteries are exhausted.

Figure 29. The AeroVironment Raven RQ-11 UAV (manufacturer's image).

Experiments have shown that the flight endurance of the Raven RQ-11 can be dramatically increased with the addition of copper indium gallium selenide (CIGS) solar cells [24]. However, these experiments placed CIGS cells only on the top surface of the main wing assembly. This was primarily due to the fact that the top of the main wing assembly presents the only large surface area that is

exposed to relatively uniform irradiance conditions. Thus, placing CIGS cells on smaller, shaded areas of the UAV (i.e., the vertical stabilizer) could significantly decrease the performance of the main wing array. Similar to previous examples, the micro-converter approach would be particularly useful due to the different surfaces of the UAV being exposed to a dynamic range of irradiance levels. This is further complicated by the constant banking and turning that occurs in flight. The use of micro-converters would allow for almost every square inch of the Raven to be covered in thin film cells resulting in multiple panels. In addition to each panel tracking its MPP independently, each DC converter could be customized to allow for greater flexibility in meeting the Raven's charging requirement of approximately 25 V. This is especially applicable to smaller areas of the Raven where arranging 48 cells in series (V_{OC} > 25 V) is not practical.

V. TEST AND DATA ANALYSIS

A. INTRODUCTION

This primary goal of testing is to evaluate the multiple MPPT approach and to validate an increase in the efficiency compared to direct loading or a central converter. The individual MPPT and solar panel selection process that was conducted prior to integrating the final PV system for testing is discussed in this chapter. Once the system was integrated, tests were carried out to evaluate the performance of the system during varying levels of irradiance under direct loading, central-converter, and micro-converter arrangements. Finally, the data was analyzed and general observations were made about the use of multiple MPPTs.

General equipment utilized throughout testing are discussed in the following subsections.

1. Amprobe Solar 600 Analyzer

The I-V and P-V characteristics of the solar panels are obtained with the Amprobe Solar-600 analyzer. This analyzer, shown in Figure 30, is a high-quality diagnostic device capable of testing and determining the operating characteristics of solar panels [24]. The solar panel being analyzed is subjected to V_{OC}, I_{SC}, and numerous operating points in between to create an exportable spread sheet of data that can be used to plot the I-V and P-V relationships. Additionally, the V_{MPP} of the panel is identified which can be used to determine if the MPPT is

properly tracking the MPP. An example of the data exported from the Solar-600 is shown in Appendix B.

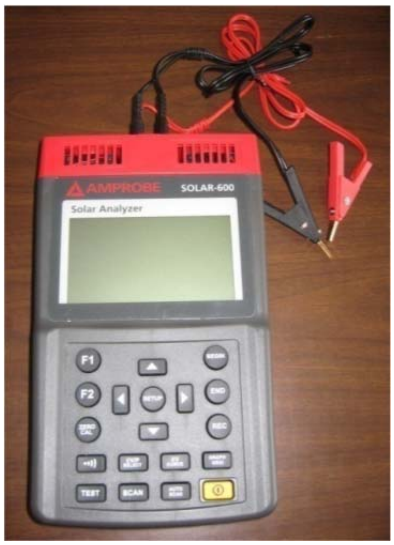

Figure 30. The Amprobe Solar-600 Analyzer (From [24]).

2. Radiant Source Technology (RST) Solar Simulator

The RST Solar Simulator is a light source for use in the testing of solar cells, sun sensors, and other small devices. The simulator, shown in Figure 31, has the following output capabilities [25]:

- Output Beam: 12” x 12”
- Lamp Power: 3000 W
- Air Mass Capability: AM0
- Cooling: Forced air
- Classification: ABA ASTM E927
  Spectral match, class A, 0.75–1.25
  Non-uniformity of irradiance, class B, ≤5%
  Temporal instability, class A, ≤2%

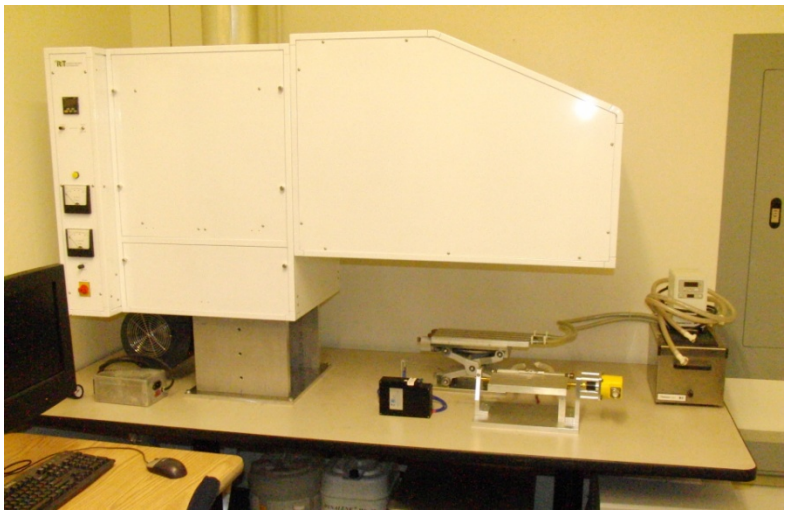

Figure 31. The RST Solar Simulator (From [25]).

3. Fluke 45 Dual Display Multimeter

The Fluke 45 is a dual-display meter that is able to display two properties of an input signal simultaneously (i.e., AC voltage and frequency). It also has the ability to sample both the voltage and current of DC signal if wired appropriately. As shown by the circuit diagram in Figure 32, two Fluke 45s were used to simultaneously monitor the input voltage and current and the output voltage and current for efficiency calculations.

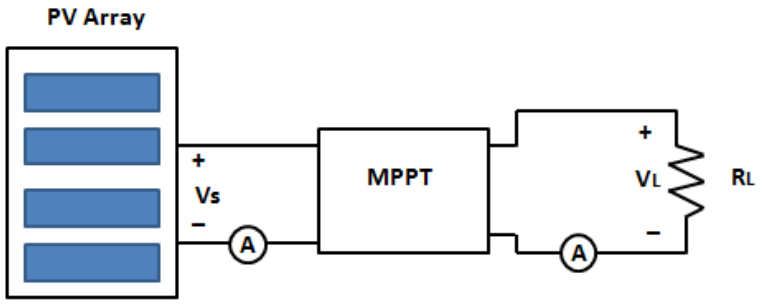

Figure 32. The input and output parameters required for efficiency calculations.

B. MPPT SELECTION

1. STEVAL SPV1020 MPPT with DC-DC Boost Converter

The STEVAL SPV1020 MPPT with a boost converter, shown in Figure 20, was initially chosen due to its advertised high efficiency (up to 98%) and its wide input voltage range (6.5 V to 45 V). It contains a modified switch-mode DC-DC boost converter, and the duty cycle is controlled by a digital P&O MPPT algorithm. Three demonstration boards (STEVAL ISV009V1) based on the SPV1020 were purchased from the manufacturer in order to design and test a distributed PV architecture similar to the set-up shown in Figure 33. An example of the external components that are required when using the SPV1020 can be found by referencing the ISV009V1 design schematic contained in Appendix A.

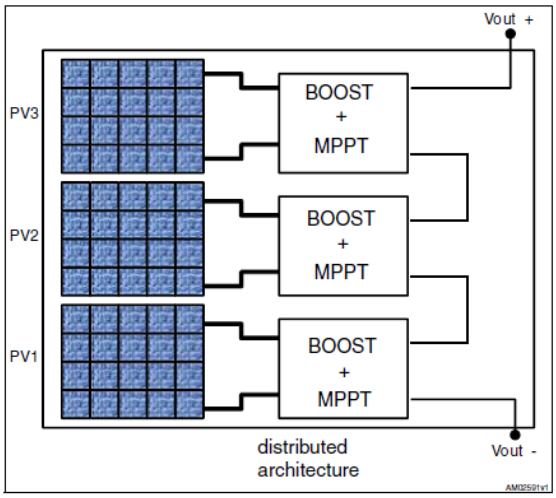

Figure 33. A distributed PV system using multiple MPPTs (From [26]).

a. STEVAL-ISV009V1 Specifications

Additional features of the ISV009V1 include:

- 300 W converter with a maximum input current of 9 A.

- Pulse-width modulation mode DC-DC boost converter with imbedded power metal–oxide–semiconductor field-effect transistors for active switches and synchronous rectification.
- Operating voltage range 6.5 V to 40 V.
- Overvoltage, overcurrent, and over temperature protection.
- Duty cycle controlled by MPPT algorithm with 0.2% accuracy.

b. ISV009V1 Testing

In order to utilize the ISV009V1 demonstration board with the available PV arrays, the input and output voltage settings were modified with the help of Mr. Ron Phelps, an electronics engineer in the Space Systems Academic Group at NPS. Specific changes included the input voltage of the ISV009V1 demonstration board (30 V) being reduced to match the approximate output voltage of the PANSAT panel ($V_{OC} \approx 19$ V). This was accomplished by modifying the input voltage divider comprised of resistances R1 and R2. Additionally, the voltage output of the demonstration board was changed from 36 V to 25.2 V by modifying the output voltage divider comprised of resistances R3 and R4. The equations that are necessary to tailor the SPV1020 to a specific application can be found in the manufacturer's AN3272 Application Note.

Once the ISV009V1 demonstration board was modified, an initial test was conducted to verify input and output voltages and check for proper MPPT algorithm functionality. The PANSAT panel, the ISV009V1 MPPT, and a fixed load were tested using the RST solar simulator. To control for the temperature effects on the PANSAT panel,

all tests were conducted by opening the shutter on the solar simulator, measuring the relevant input and output readings, and then closing the shutter which kept the solar panel near room temperature (~72 F).

The characteristic I-V curve of the PANSAT panel is shown in Figure 34, and a V_{MPP} of 11.97 V was identified using the Solar-600 analyzer. As shown in Table 3, the load on the system was systematically increased until the efficiency of the system reached 76%. Any attempts to increase the load past this point resulted in the ISV009V1 MPPT producing erratic, fluctuating voltage levels on both the input and output. Prior to reaching this point of instability, the MPPT operating point was constantly 2 V higher than the V_{MPP}, and the output voltage remained within 1.3 V of the desired 25.2 V output. All three demonstration boards displayed similar erratic behavior once the 76% efficiency threshold was exceeded.

Table 3. Using PANSAT array, the results of a systematic increasing of the load with the ISV009V1 MPPT.

Resistance (Ω)	**V_{MPPT} (V)**	**I_{MPPT} (mA)**	**V_{load} (V)**	**I_{load} (mA)**	**η**
488	16.6	97.7	24.8	49.4	75.9%
377	14.3	168.3	26.43	67.9	74.7%
300	----------UNSTABLE----------				

The test was repeated outside with a CIGS array that produces approximately 8 W compared to the PANSAT's 2.5 W. Although a minimum power input is not mentioned in the data sheet, a larger array was chosen to ensure there is not a minimum wattage rating for the ISV009V1 MPPT that may have caused the instability. The V_{MPP} of the CIGS array is 8.25 V as determined by the Solar-600 analyzer. As shown in Table

4, a larger range of resistance values is used to ensure the load power plus the conversion losses of the MPPT did not exceed the power output of the array which likely causes the instability. Prior to reaching the point of instability, the MPPT operating point was at least 7.5 V higher than the V_{MPP}, and the output voltage fluctuated 2 V over the desired 25.2 V.

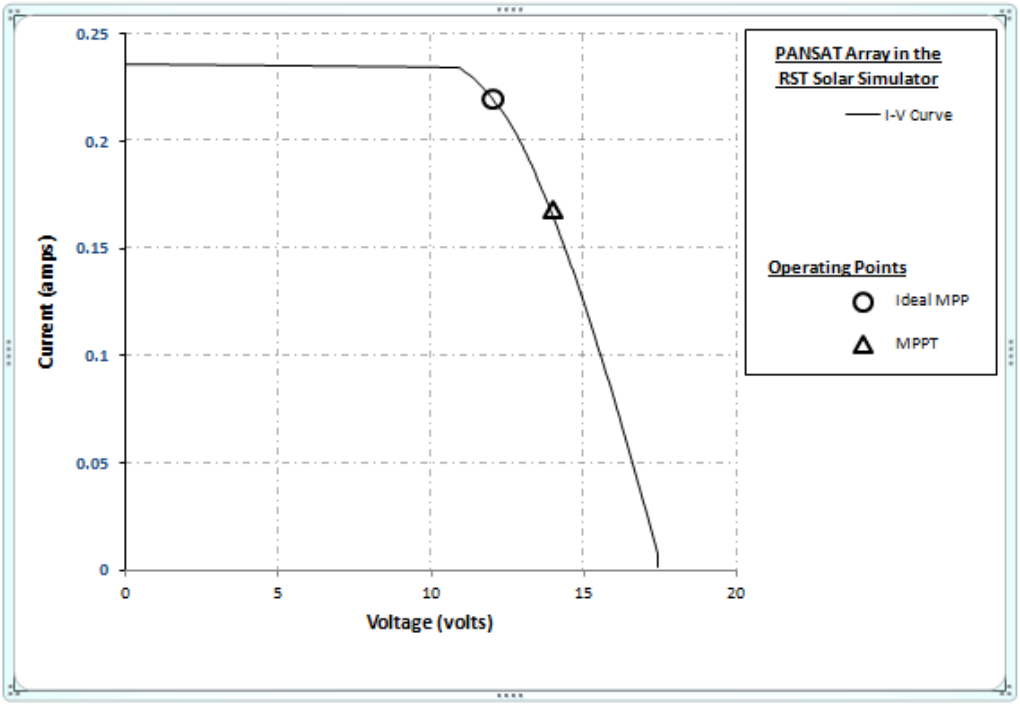

Figure 34. The actual MPP versus the ISV009V1 MPPT operating point of the PANSAT array in the RST solar simulator.

c. ISV009V1 Demo Board Test Conclusions

The primary problem with the ISV009V1 is the poor performance in tracking the V_{MPP} of the array it was paired with. This large tracking error meant the array was not operating near its maximum potential, thus, making the subsequent efficiency of the DC-DC converter irrelevant for

purposes of this thesis. Additional concerns include the unpredictable behavior once the point of instability was exceeded and the inability of the ISV009V1 in maintaining a constant 25.2 V output.

The problems with the ISV009V1 were not resolved and, therefore, it was not used for the final PV system design. Possible explanations of the instability include:

- While replacing resistors R1 through R4, Mr. Phelps also soldered several unconnected output pins of the SPV1020. According to the manufacturer's AN3272 Application Note, all pins of the SPV1020 served a specific function. These unconnected pins may indicate a questionable build quality of the demonstration board.
- Although not specifically mentioned by the manufacturer, the SPV-1020 may not be designed to directly power a load as done in this test. The SPV-1020 may require an appropriate battery charger such as the STEVAL SEA05 battery controller.

Table 4. Using the CIGS array, the results of a systematic increasing of the load with the ISV009V1 MPPT.

Resistance (Ω)	**V_{MPPT} (V)**	**I_{MPPT} (mA)**	**V_{load} (V)**	**I_{load} (mA)**	**η**
4.7k	17.5	15.9	27.5	5.8	57.5%
1.5k	17.1	40.1	27.1	17.6	69.1%
488	16.5	92.3	23.9	47.5	74.8%
300	15.7	171.8	25.1	80.1	74.8%
200	15.1	220.0	25.1	116.0	87.7%
177	15.1	220.0	23.5	122.0	86.0%
164	14.91	242.0	23.9	134.7	89.2%
135	----------UNSTABLE----------				

2. Genasun-4 MPPT with DC-DC Buck Converter

The Genasun-4 was chosen to replace the ISV009V1 due to its proven performance when used on a prior thesis. To

conduct the initial tests, the PANSAT array, the Genasun-4 MPPT, a three cell lithium-ion battery, and a fixed resistive load were arranged as shown in Figure 35.

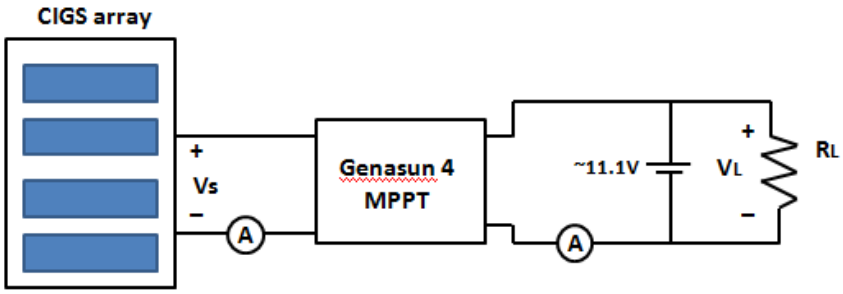

Figure 35. Circuit diagram of the Genasun-4 test set-up.

a. Genasun-4 Specifications

The Genasun-4, shown in Figure 36, is originally designed to be used with lead-acid batteries with a float voltage of 13.8 V. However, the manufacturer modified the MPPTs by reducing the float voltage to 12.5 V for use with three cell lithium-ion batteries. Additional specifications include:

- Maximum Panel Power: 50 W
- Rated Output Current: 4 A
- Panel Voltage (V_{OC}): 0–27 V (however, must be greater than the battery voltage to charge)
- Digital P&O algorithm that controls the duty cycle of an inductively fed, switch mode buck DC-DC converter
- Tracking efficiency: 99% typical
- Overall Efficiency: 94% to 99.85% typical

Figure 36. The Genasun-4 MPPT with DC-DC buck converter and charge controller.

b. Genasun-4 Testing

The Genasun-4 was paired with a CIGS array and tested outdoors. Full irradiance and two degradations of irradiance were tested by shading six of the 48 cells within the array as shown in Figure 37. The effects of temperature were reasonably controlled by allowing the array to reach a relatively constant temperature of 105 F. The goal of testing was to verify the effectiveness of the P&O algorithm and calculate the MPPT's efficiency.

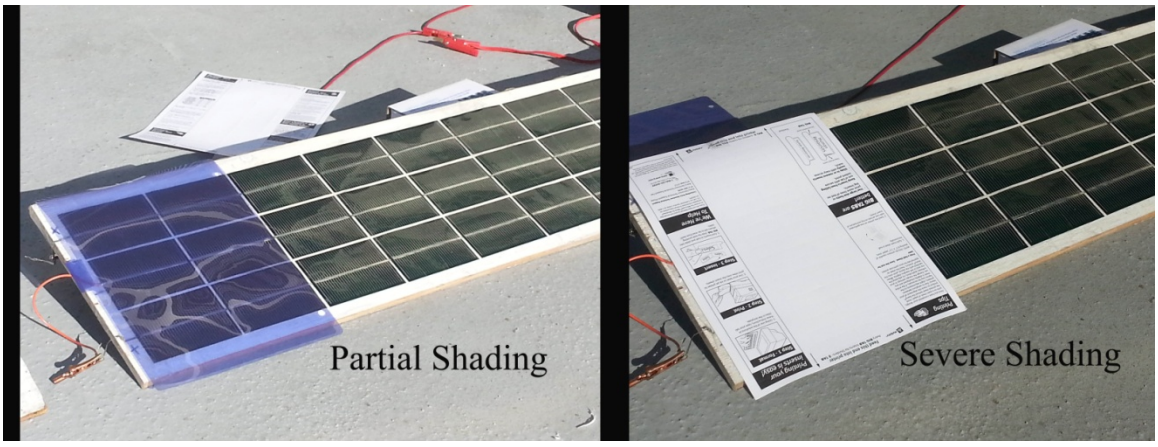

Figure 37. The methods used to simulate partial and severe shading of the CIGS array.

The operating points of the Genasun-4 test are shown in Figure 38. The shifting value of the V_{MPP} in varying irradiance conditions and the subsequent performance of the Genasun-4 can be seen in Table 5.

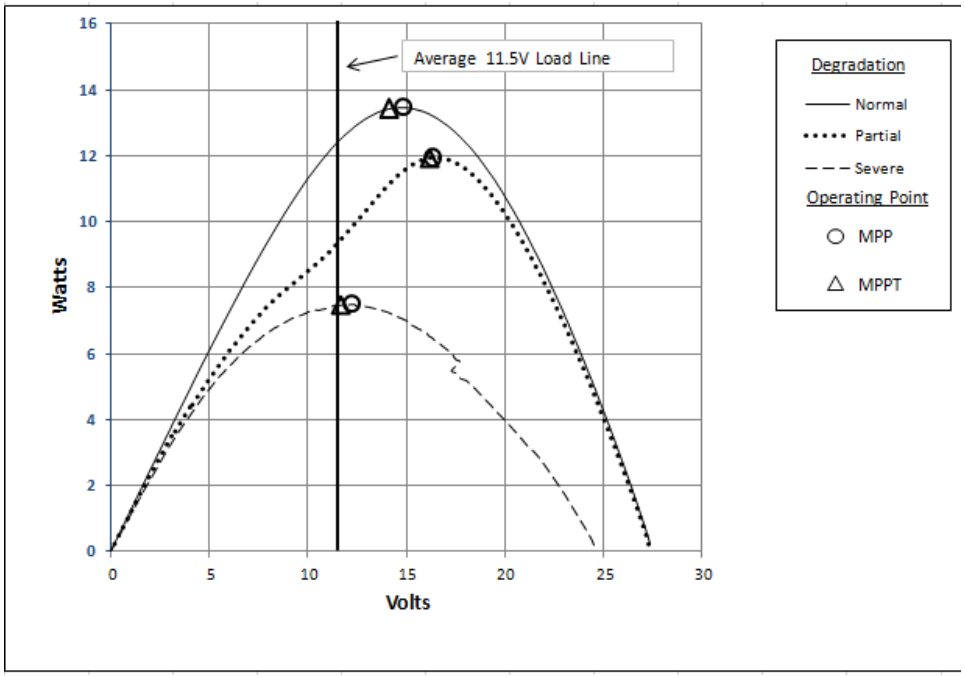

Figure 38. The resulting P-V curves of a CIGS array subjected to varying irradiance levels with MPP and MPPT operating points depicted.

Table 5. The test results of the Genasun-4 MPPT.

Shading	Solar Analyzer		MPPT		Output		Efficiency
	V_{MPP} (V)	I_{MPP} (A)	V_{MPPT} (V)	I_{MPPT} (A)	V_{load} (V)	I_{load} (A)	η in %
Normal	14.81	0.91	14.41	0.93	11.65	1.11	95.9%
Partial	16.30	0.73	16.20	0.73	11.58	0.98	95.4%
Severe	12.23	0.62	11.84	0.64	11.32	0.65	97.1%

c. Genasun-4 MPPT Test Results

The performance of the Genasun-4 MPPT closely matched manufacturer specifications. Specifically, the tracking algorithm had a tracking efficiency between 97-

99%. The total conversion efficiency (i.e., the tracking error and DC-DC conversion losses are subtracted) ranged between 95-97%. The load voltage averaged 11.52 V with fluctuations less than 0.2 V. Due to the accuracy of the MPPT algorithm and the high overall system efficiency, the Genasun-4 was selected for use in the final system design.

C. SOLAR PANEL SELECTION

The selection of the two solar panels was primarily influenced by the Genasun-4 MPPT specifications. The array requirements that must be satisfied include:

- V_{OC} cannot exceed 27 V.
- The power of all panels combined cannot exceed 50 W.
- The charging voltage must always exceed the battery voltage.

The first panel that met most of the requirements was the PANSAT panel. However, during the ISV00091 MPPT testing, we discovered that the PANSAT panel has a V_{MPP} of 11.97 V as depicted in Figure 34. This was determined to be a problem since the test plan called for significantly degrading the irradiance levels which causes the V_{MPP} to drop. Since the battery voltage range is between 8.1 to 12.5 V, the MPPT algorithm will not track the MPP once the V_{MPP} of the array drops below the battery voltage. To ensure the V_{MPP} would always exceed the battery float voltage of 12.5 V, a DC voltage source of 5.0 V was placed in series with the PANSAT panel, and new V_{MPP} of 16.97 V was obtained. This technique maintains the shape of the characteristic I-V curve with the exception of shifting it to the right by 5.0 V.

The second panel that was used for testing included two strings of the degraded CIGS array (i.e., 32 cells in series). Only two strings were selected to prevent the V_{OC} of the CIGS array from exceeding the Genasun's maximum input voltage of 27 V. The CIGS panel had a V_{MPP} of 6.6 V, which is well below the battery voltage range. Thus, for similar V_{MPP} concerns previously mentioned with the PANSAT panel, a DC voltage source of 9.8 V was placed in series with the CIGS panel to give a new V_{MPP} of approximately 16.4 V.

D. FINAL DESIGN

The final design of the solar panels and MPPTs supported three test scenarios. First, the panels would be tested in the direct loading approach as shown in Figure 39.

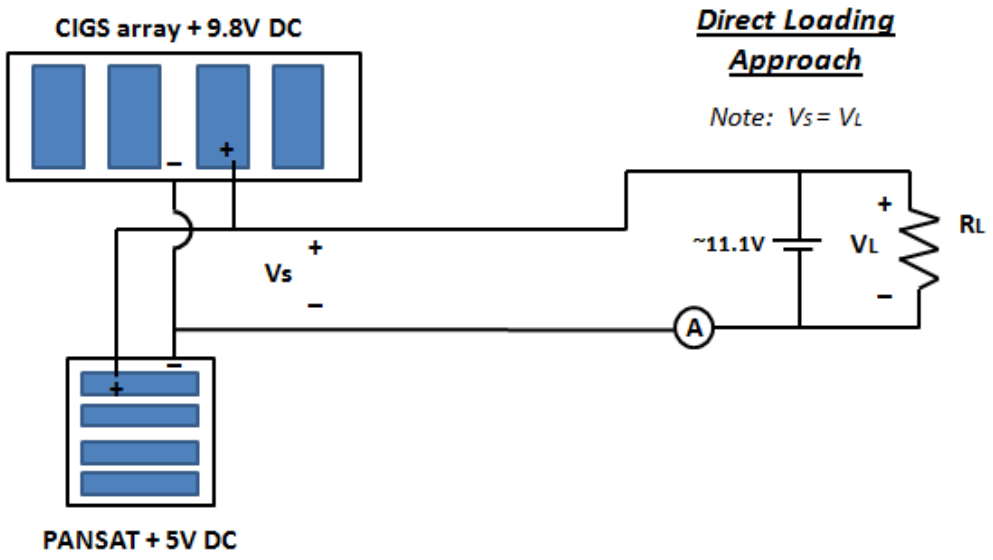

Figure 39. Circuit schematic for the direct loading approach.

Then, the central converter approach would be tested as shown in Figure 40.

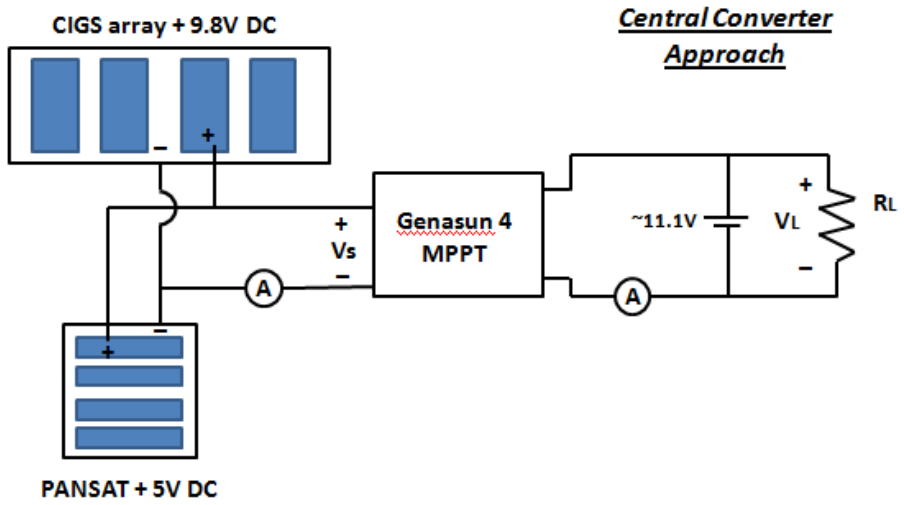

Figure 40. The circuit schematic for the central converter approach.

Finally, the micro-converter approach would be tested as shown in Figure 41.

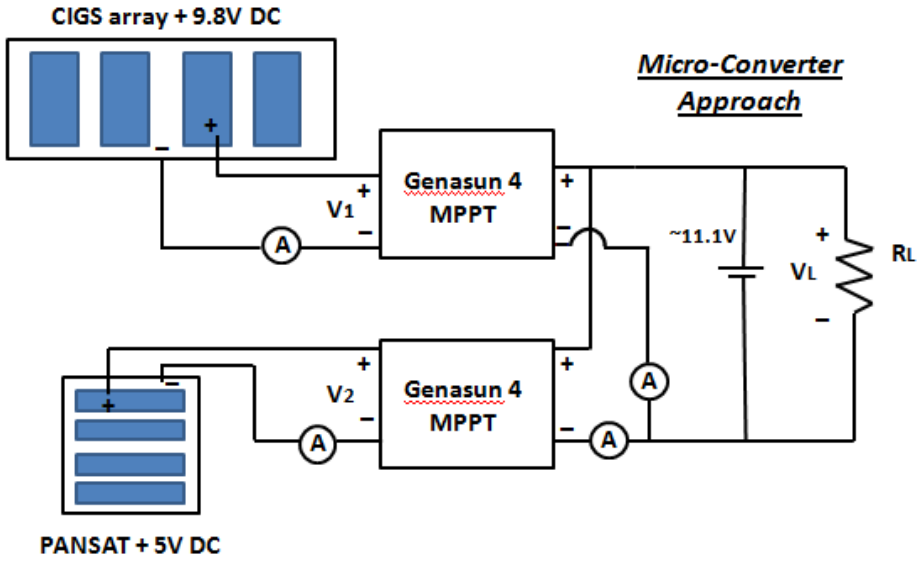

Figure 41. The circuit schematic for the micro-converter approach.

An image of the actual equipment used is shown in Figure 42.

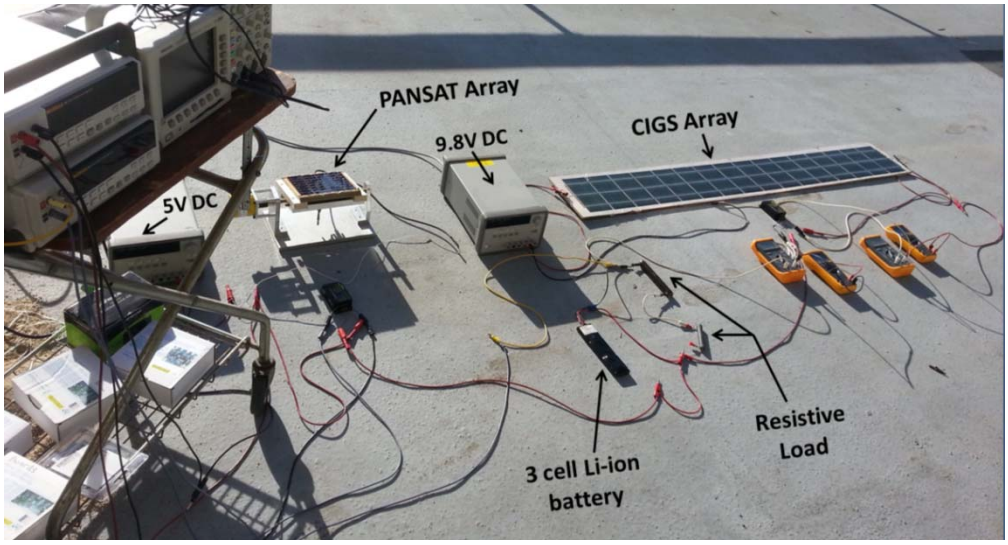

Figure 42. The primary equipment used to conduct the tests.

E. DATA

Varying the levels of irradiance was accomplished by independently tilting the arrays at approximated angles from the sun. For example, the 0°/30° position means the CIGS wing was normal to the sun, and the PANSAT was offset by approximately 30 degrees. For each position, the three test scenarios were implemented, and the relevant voltage and current values were recorded. The I-V curves for each array configuration and the operating points of the direct loading, central converter, and micro-converter tests are graphically depicted in Appendix C. Although the individual test data points in Appendix C and the following tables are relevant, a summary of the power delivered to the loads and MPPT efficiency is shown in Table 10 and can be used as the primary reference when drawing conclusions.

The results for the direct loading tests for the different irradiance levels are summarized in Table 6.

Table 6. Data points for the direct load tests.

Direct Loading	Panel 1||2 CIGS+PANSAT		MPPT Operating Point		Load		Power		
Panel Configuration	V_{MPP} (V)	I_{MPP} (A)	V_{MPPT} (V)	I_{MPPT} (A)	V_{Load} (V)	I_{Load} (A)	P_{MPP} (W)	P_{MPPT_In} (W)	P_{Load} (W)
0°/0°	14.82	1.43	--	--	11.62	1.65	21.19	--	19.17
30°/0°	15.75	1.03	--	--	11.54	1.19	16.22	--	13.73
0°/30°	14.43	1.46	--	--	11.47	1.68	21.07	--	19.27
0°/60°	14.25	1.47	--	--	11.47	1.71	20.95	--	19.61
60°/0°	17.82	0.30	--	--	11.41	0.34	5.35	--	3.88
60°/60°	17.45	0.32	--	--	11.40	0.37	5.58	--	4.22

The results for the central converter tests for the different irradiance levels are summarized in Table 7.

Table 7. Data points for the central converter tests (an asterisk indicates an error in determining the MPP as discussed in section F.5 of this chapter).

Central Converter	Panel 1||2 CIGS+PANSAT		MPPT Operating Point		Load		Power		
Panel Configuration	V_{MPP} (V)	I_{MPP} (A)	V_{MPPT} (V)	I_{MPPT} (A)	V_{Load} (V)	I_{Load} (A)	P_{MPP} (W)	P_{MPPT_In} (W)	P_{Load} (W)
0°/0°	14.82	1.43	14.90	1.66	11.98	1.94	21.19	24.73 *	23.24
30°/0°	15.75	1.03	15.60	1.30	11.93	1.62	16.22	20.28 *	19.33
0°/30°	14.43	1.46	14.90	1.60	11.94	1.86	21.07	23.84 *	22.21
0°/60°	14.25	1.47	15.60	1.10	11.84	1.36	20.95	17.16	16.10
60°/0°	17.82	0.30	16.20	0.33	11.80	0.43	5.35	5.35	5.07
60°/60°	17.45	0.32	17.50	0.33	11.75	0.47	5.58	5.78 *	5.52

The micro-converter voltage and current readings are summarized in Table 8.

Table 8. Voltage and current readings for the micro-converter tests (an asterisk indicates a "bypass" mode as discussed in Section F.4 of this chapter).

Micro-converter	MPP Panel 1 (CIGS)		MPPT 1 Operating Point		Load 1		MPP Panel 2 (PANSAT)		MPPT 2 Operating Point		Load 2	
Panel Configuration	V_{MPP} (V)	I_{MPP} (A)	V_{MPPT} (V)	I_{MPPT} (A)	V_{Load} (V)	I_{Load} (A)	V_{MPP} (V)	I_{MPP} (A)	V_{MPPT} (V)	I_{MPPT} (A)	V_{Load} (V)	I_{Load} (A)
0°/0°	15.15	1.34	14.75	1.33	11.9	1.58	16.44	0.25	16.56	0.24	11.9	0.31
30°/0°	16.27	0.97	16.00	0.98	11.90	1.25	16.44	0.25	16.47	0.24	11.9	0.31
0°/30°	15.15	1.34	14.9	1.36	11.83	1.58	17.24	0.17	17.30	0.17	11.8	0.21
0°/60°	15.15	1.34	15.2	1.37	11.84	1.63	17.26	0.03	11.8*	0.04	11.8	0.04
60°/0°	18.24	0.32	17.9	0.31	11.74	0.44	16.08	0.24	15.93	0.24	11.7	0.30
60°/60°	18.24	0.32	17.9	0.32	11.70	0.46	17.26	0.03	11.7*	0.04	11.7	0.04

The micro-converter power calculations are contained in Table 9.

Table 9. Power calculations for the micro-converter tests.

Micro-converter	Power		
Panel Configuration	P_{MPP} (W)	P_{MPPT_In} (W)	P_{Load} (W)
0°/0°	24.33	23.61	22.54
30°/0°	19.81	19.70	18.61
0°/30°	23.25	23.21	21.18
0°/60°	20.89	21.27	19.73
60°/0°	9.75	9.37	8.69
60°/60°	6.46	6.16	5.80

Table 10. A power and overall system efficiency analysis for the three test scenarios (an asterisk indicates an MPP tracking error as discussed in Section F.5 of this chapter).

Power Delivered/Overall Efficiency	Power (W) / (Efficiency %)		
Panel Configuration	Direct Loading	Central Converter	Micro-inverter
0°/0°	19.17 / (n/a)	23.24 / (94 % *)	22.54 / (93%)
30°/0°	13.73 / (n/a)	19.33 / (95% *)	18.61 / (94%)
0°/30°	19.27 / (n/a)	22.21 / (93% *)	21.18 / (91%)
0°/60°	19.61 / (n/a)	16.10 / (94%)	19.73 / (94%)
60°/0°	3.88 / (n/a)	5.07 / (95%)	8.69 / (89%)
60°/60°	4.22 / (n/a)	5.52 / (99 % *)	5.80 / (90%)

F. OBSERVATIONS

1. MPPTs Outperform the Direct Loading Approach

As shown in Table 10, the power delivered to the load when using either one or two MPPTs almost always exceeded the direct loading method. The one abnormality occurred in the $0^o/60^o$ test between the direct loading and central converter methods. Possible explanations include operator error or equipment malfunction.

2. Micro-inverters Versus Central Converter

The primary advantage of using micro-inverters vice a central converter is apparent when the arrays encountered extreme differences in the levels of irradiance. This observation can be seen by referring to Table 10 and comparing the power delivered when the difference in irradiance levels was relatively similar (i.e., 30^o or less) and when they were drastically different (i.e., 60^o between arrays). The micro-converter approach delivered significantly more power than the central converter method in both the $0^o/60^o$ and $60^o/0^o$ tests. However, when the micro-

converter method is compared to direct loading in the 0°/60° test, the minor gain in power delivered would appear to contradict this observation. This incongruity is a result or a more linear I-V curve that is caused by using a degraded CIGS array. The relationship between an array's FF and the use of MPPTs is discussed further in the final chapter.

A disadvantage to using micro-inverters versus a central converter can be seen in Table 10 by comparing the power delivered when the arrays experienced similar irradiance conditions. In the 0°/0°, 30°/0°, and the 0°/30° configurations, the power delivered to the load was significantly less than the central converter method.

3. Tracking Accuracy

The P&O algorithm took approximately five seconds to transition from V_{OC} operating point to its self-calculated V_{MPPT}. When calculating the tracking accuracy, the two severe degradations of the PANSAT panel (i.e., the 0°/60° and 60°/60° configurations) in the micro-converter tests were omitted due to a "bypass" mode being triggered by the Genasun-4. Excluding those two test points, the Genasun-4 averaged a 98% tracking accuracy.

4. Bypass Mode

The bypass mode can be identified when the Genasun's input operating points mirror the load voltage and current. In other words, the MPPT appears to recognize when certain design limitations have been reached and allows array output power to be directly delivered to the load by passing through the MPPT. This mode is indicated by the use

of asterisks in Table 8. The pass-through mode can be identified by comparing the voltage and current values when the PANSAT array is severely degraded (i.e., the 60^{o} position). These two specific scenarios appear to activate the bypass mode for different reasons. The first scenario is when the current level is such a small value that perturbations in the operating point yield no measurable gain or loss in the array's power. This would mean the P&O tracking algorithm has difficulty in locating the V_{MPP} due to a flattened P-V curve. In the second scenario, the MPPT activates the bypass mode when the V_{MPP} drops below the charging voltage. As stated in the product specifications, the array voltage must be higher than the battery voltage in order to charge.

While the bypass mode may not be as significant to some applications, this design feature increased the power delivered to the load by approximately 2.5% in these two scenarios. The manufacturer's decision to include a bypass mode vice shutting down the MPPT when certain design limitations have been exceeded is a desirable attribute. On a side note, the manufacturer does not specifically mention this mode of operation, thus, the term "bypass" is used for lack of a more proper term.

5. MPP error during central converter test

As shown by the use of asterisks in Table 7 during the central converter tests, the MPPT operating point during four of the six irradiance configurations resulted in a power calculation that far exceeded the MPP as measured by the Solar-600 analyzer. The central converter tests were the only time during testing the MPPT produced more power

than the Solar-600 analyzer's estimation of the actual MPP. Reasons for this error are not understood.

THIS PAGE INTENTIONALLY LEFT BLANK

VI. CONCLUSIONS

The PV system designer has many options available if they choose to build their own MPPT. However, the decision to utilize a commercially available MPPT will most likely result in a digital microprocessor with a P&O or slightly modified P&O algorithm. These commercial P&O MPPTs are efficient, reliable, and becoming extremely affordable. However, their primary disadvantage resides in the P&O tracking algorithm. Depending on how far the MPP shifts due to changing environmental conditions, the P&O algorithm can take up to 2.6 seconds or longer to successfully change the array's operating point to the new MPP. It is this author's opinion that the digital P&O MPPTs currently available in the commercial market will successfully meet the performance specifications of most Department of Defense (DoD) solar applications. A slight increase in expense might be encountered in order to meet the reliability and durability requirements of the military. However, the dynamic environment that the military operates is where this research has concluded the multiple MPPT approach works best and a slight expense may be worthwhile.

For specialized applications that require a faster tracking response time (i.e., a rotating satellite), the PV system designer should consider more advanced algorithms such as fuzzy logic and neural networks. While not discussed in depth in this research, these advanced algorithms can learn from past behavior and are able to effectively respond to nonlinear inputs such as rapidly changing environmental conditions. However, these advanced

algorithms require more processing power to implement and are cost prohibitive for most commercial applications.

Finally, the emergence of efficient analog MPPT algorithms combined with the promising research into capacitively fed, switch-mode converter technologies presents the best option for realizing the ideal, per cell application of MPPTs. This distributed PV architecture would be extremely beneficial as each cell could be optimized to perform at the MPP despite manufacturing irregularities, local environmental degradations, or cell damage.

The remaining sections in this chapter are a summary of primary conclusions that resulted from this research and recommendations are made for future work.

A. CONCLUSIONS

1. MPPT Versus Direct-Loading

The results showed that in every test configuration, the central converter and micro-converter approach outperformed direct loading. Although this conclusion might be considered predictable due to numerous academic studies and a successful MPPT commercial market, the author found that DoD solar applications typically rely on direct-loading vice using MPPTs. The reason behind this has its advantages; a well-designed, directly-loaded PV system will have a MPP near or slightly above the load voltage. This results in a simple, reliable, and for most applications, a cost-effective PV system. However, as validated in this research, a slight shift in the MPP due to environmental conditions has a substantial effect on the power output of

the array. With consideration to the reliability and affordability of modern MPPTs, there should be at a minimum of one MPPT per PV system for DoD applications that are subjected to dynamic operating conditions (i.e., solar blankets or UAVs).

2. Multiple MPPT Performance

The multiple MPPT approach provided the most benefit when the two panels experienced drastically different irradiance levels (i.e, 60^{o} of tilt). This research mirrored the advertised claims of the micro-inverter manufacturers. In particular, it was seen that localized disruptions disproportionately affect the output power of the entire array. However, it was also noticed that the micro-converter approach was on par with the central converter configuration when the PV system experienced slight variations of irradiance (i.e., 30^{o} or less). Thus, the term "localized disruption" is ambiguous, and the factors that determine at which point the micro-converter approach outperforms the central converter configuration was not resolved with this research.

3. FF Versus MPPT Performance

Arrays with a poor FF are not a great candidate for MPPTs. This conclusion was first noticed when analyzing the results from the initial Genasun-4 MPPT testing. According to the Solar-600 analyzer, the degraded CIGS array had a very low fill factor (i.e., approximately 38%). Due to the linear I-V curve that results from a poor FF, changes in the operating point yield nominal increases or decreases in power. This can be graphically depicted in Figure 43 where

the I-V curves of a degraded CIGS array, a newer CIGS array, and a traditional silicone array is compared. It can be seen that for the same 3.0 V shift towards the MPP that is applied to both the degraded CIGS (i.e., point A to B) and the silicon panel (i.e., point C to D), a drastically different power output is achieved. This can be seen graphically by comparing the size of the rectangles that exist between the two operating points for each I-V curve. The power represented by the rectangles at point A and B are approximately equal in size. Thus, due to the linear I-V curve caused by the poor FF of the degraded CIGS array, shifting the operating point only yielded a gain of 12%. However, the same 3.0 V shift with the silicon array yields a significant increase (i.e., approximately 50%) in power as graphically depicted by the larger rectangle created by operating at point D vice point C.

Common explanations for a poor FF include inferior quality, degradation due to age, or cell damage. Regardless of the reason, this research has concluded that cells with a poor FF will see at best, a slight increase in output power when paired with one or multiple MPPTs. In particularly low FF arrays (i.e., less than 40%), the increase was relatively insignificant.

B. RECOMMENDATIONS FOR FUTURE WORK

1. A More Refined Method in Validating the Nultiple MPPT Approach

The ability to precisely control the changes in environmental conditions would provide for a more accurate performance characterization for all three test configurations (i.e., direct-loading, central-converter,

and micro-converter). Recommendations include modeling the system and/or ensuring the PV panels utilized can fit inside the solar simulator. Additionally, a more sophisticated PV system that is comprised of more than two panels could provide further insight into how the system behaves when exposed to a wider range of environmental conditions.

2. Design of a "Per Cell" MPPT

With the recent advances in tracking algorithms that require relatively few parts (i.e., analog TEODI or small microprocessors) combined with highly efficient and increasingly smaller converters, an MPPT could be designed to be applied to each individual cell within an array. This research would be challenging due to the lack of space available on solar arrays. However, the recent advancements in MPPT technology has made this concept worth further investigation.

3. Capacitor-Based Converter Technologies

Relatively heavy, switch-mode converters are used in almost all portable electronics. Research into a lighter and smaller technology that replaces inductively fed converters would have benefits that extend well beyond MPPTs.

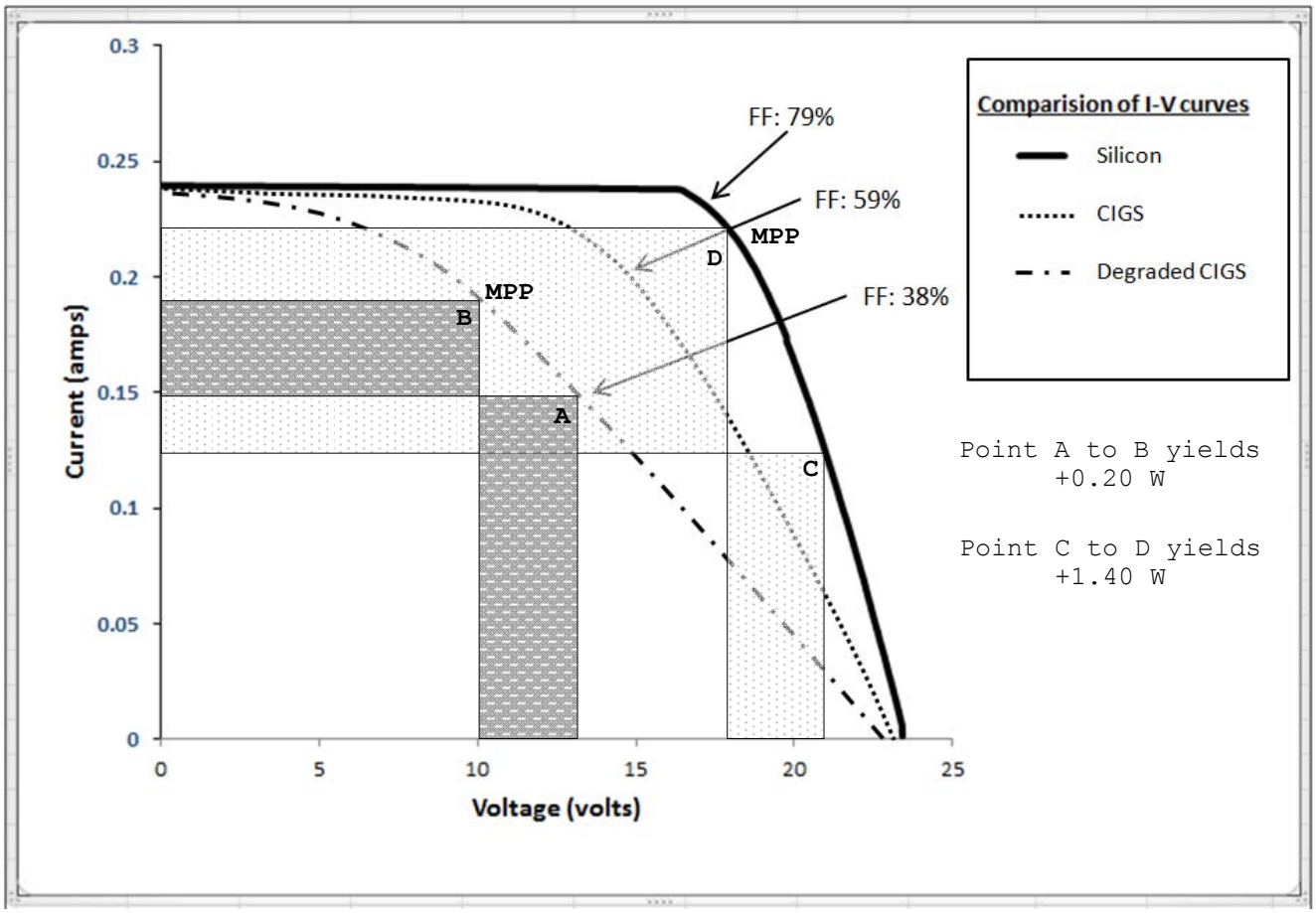

Figure 43. A visual representation of how a poor FF adversely affects MPPT performance.

APPENDIX A. STEVAL ISV009V1 SCHEMATIC

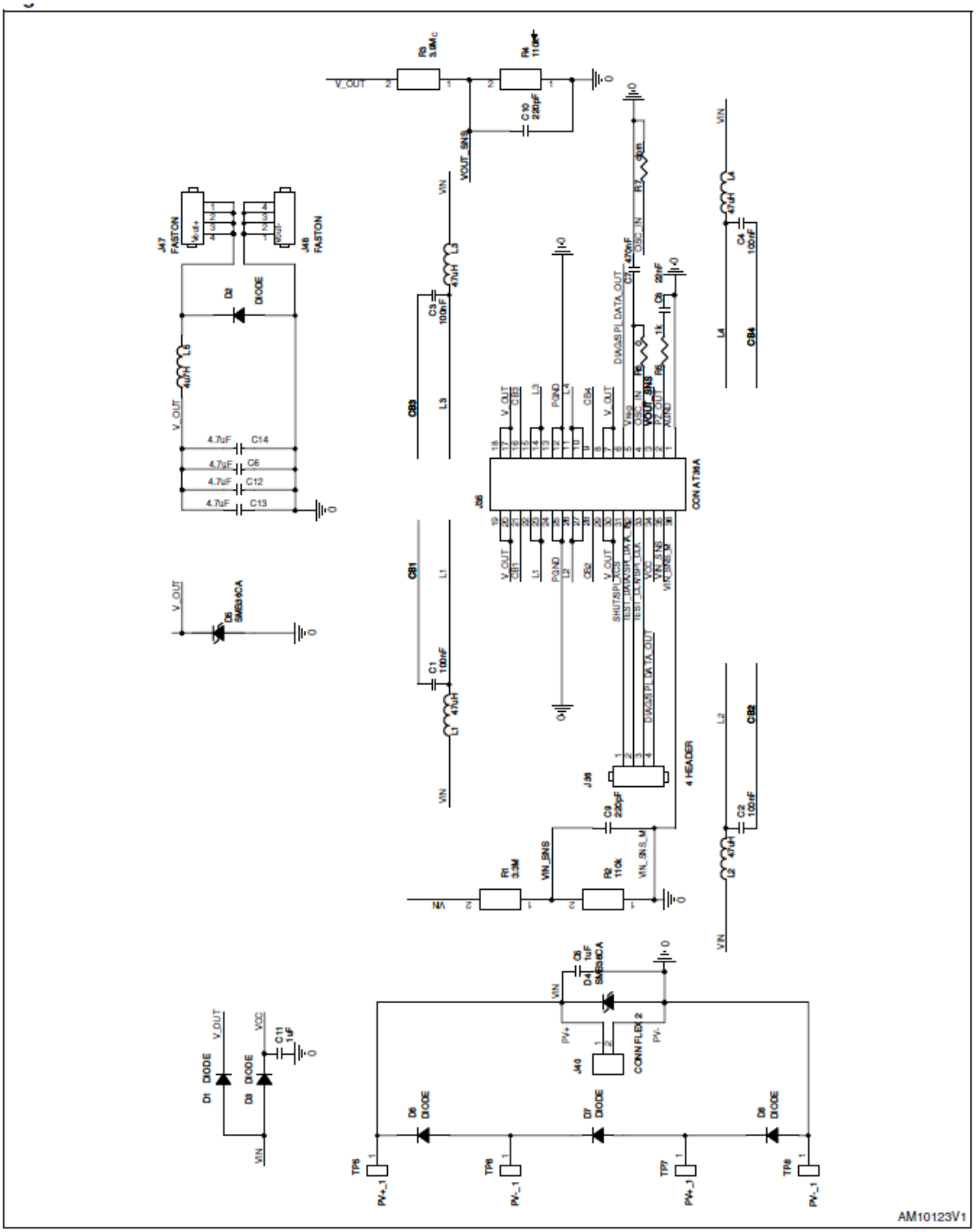

THIS PAGE INTENTIONALLY LEFT BLANK

APPENDIX B. AMPROBE SOLAR-600 ANALYSIS EXAMPLE

Sample No. 48	PANSAT Silicon	
Date & Time	--	
Vopen (V)	19.43	
Ishort (A)	0.265	
Vmaxp (V)	13.54	
Imaxp (A)	0.247	
Pmax (W)	3.357	
V (V)	I (A)	P (W)
19.454	0.0016	0.031126
19.45	0.0034	0.06613
19.447	0.0052	0.101124
19.446	0.007	0.136122
19.417	0.0088	0.17087
19.382	0.0106	0.205449
19.348	0.0122	0.236046
19.315	0.014	0.27041
19.275	0.0158	0.304545
19.241	0.0176	0.338642
19.206	0.0194	0.372596
19.174	0.0212	0.406489
19.136	0.023	0.440128
19.106	0.0246	0.470008
19.07	0.0264	0.503448
19.037	0.0282	0.536843
18.999	0.03	0.56997
18.966	0.0318	0.603119
18.933	0.0336	0.636149
18.902	0.0354	0.669131
18.868	0.037	0.698116
18.835	0.0388	0.730798
18.802	0.0406	0.763361
18.768	0.0424	0.795763
18.736	0.0442	0.828131
18.698	0.046	0.860108

V (V)	I (A)	P (W)
18.665	0.0478	0.892187
18.631	0.0494	0.920371
18.597	0.0512	0.952166
18.563	0.053	0.983839
18.53	0.0548	1.015444
18.497	0.0566	1.04693
18.462	0.0584	1.078181
18.424	0.0602	1.109125
18.389	0.0618	1.13644
18.359	0.0636	1.167632
18.326	0.0654	1.19852
18.295	0.0672	1.229424
18.261	0.069	1.260009
18.228	0.0708	1.290542
18.194	0.0724	1.317246
18.161	0.0742	1.347546
18.123	0.076	1.377348
18.087	0.0778	1.407169
18.046	0.0796	1.436462
18.01	0.0814	1.466014
17.972	0.0832	1.49527
17.938	0.0848	1.521142
17.902	0.0866	1.550313
17.866	0.0884	1.579354
17.828	0.0902	1.608086
17.794	0.092	1.637048
17.758	0.0938	1.6657
17.723	0.0956	1.694319
17.684	0.0972	1.718885
17.648	0.099	1.747152
17.612	0.1008	1.77529
17.578	0.1026	1.803503
17.539	0.1044	1.831072
17.504	0.1062	1.858925
17.468	0.108	1.886544
17.434	0.1096	1.910766

V (V)	I (A)	P (W)
17.395	0.1114	1.937803
17.358	0.1132	1.964926
17.322	0.115	1.99203
17.284	0.1168	2.018771
17.244	0.1186	2.045138
17.207	0.1204	2.071723
17.169	0.122	2.094618
17.134	0.1238	2.121189
17.092	0.1256	2.146755
17.059	0.1274	2.173317
17.021	0.1292	2.199113
16.985	0.131	2.225035
16.942	0.1328	2.249898
16.904	0.1344	2.271898
16.862	0.1362	2.296604
16.824	0.138	2.321712
16.786	0.1398	2.346683
16.746	0.1416	2.371234
16.707	0.1434	2.395784
16.669	0.145	2.417005
16.627	0.1468	2.440844
16.588	0.1486	2.464977
16.548	0.1504	2.488819
16.509	0.1522	2.51267
16.472	0.154	2.536688
16.428	0.1558	2.559482
16.39	0.1574	2.579786
16.347	0.1592	2.602442
16.308	0.161	2.625588
16.264	0.1628	2.647779
16.223	0.1646	2.670306
16.181	0.1664	2.692518
16.138	0.1682	2.714412
16.096	0.1698	2.733101
16.05	0.1716	2.75418
16.008	0.1734	2.775787

V (V)	I (A)	P (W)
15.966	0.1752	2.797243
15.919	0.177	2.817663
15.877	0.1788	2.838808
15.833	0.1806	2.85944
15.788	0.1822	2.876574
15.739	0.184	2.895976
15.684	0.1858	2.914087
15.638	0.1876	2.933689
15.595	0.1894	2.953693
15.551	0.1912	2.973351
15.504	0.193	2.992272
15.459	0.1946	3.008321
15.412	0.1964	3.026917
15.364	0.1982	3.045145
15.314	0.2	3.0628
15.262	0.2018	3.079872
15.212	0.2036	3.097163
15.163	0.2052	3.111448

V (V)	I (A)	P (W)
15.11	0.207	3.12777
15.055	0.2088	3.143484
15.035	0.2106	3.166371
14.985	0.2124	3.182814
14.928	0.2142	3.197578
14.867	0.216	3.211272
14.81	0.2176	3.222656
14.748	0.2194	3.235711
14.687	0.2212	3.248764
14.618	0.223	3.259814
14.555	0.2248	3.271964
14.49	0.2266	3.283434
14.422	0.2284	3.293985
14.356	0.23	3.30188
14.284	0.2318	3.311031
14.212	0.2336	3.319923
14.149	0.2354	3.330675
14.075	0.2372	3.33859

V (V)	I (A)	P (W)
13.988	0.239	3.343132
13.902	0.2408	3.347602
13.823	0.2424	3.350695
13.736	0.2442	3.354331
13.64	0.246	3.35544
13.548	0.2478	3.357194
13.428	0.2496	3.351629
13.325	0.2514	3.349905
13.212	0.2532	3.345278
13.095	0.2548	3.336606
12.955	0.2566	3.324253
12.815	0.2584	3.311396
12.672	0.2602	3.297254
12.48	0.262	3.26976
12.241	0.2638	3.229176
0	0.2656	0

APPENDIX C. TEST RESULTS

The following figures are a graphical representation of the data obtained by the Solar-600 analyzer for the three different test configurations under varying levels of irradiance. The results for the 0°/0° irradiance level are shown in Figure 44. The results for the 30°/0° irradiance level are shown in Figure 45. The results for the 0°/30° irradiance level are shown in Figure 46. The results for the 0°/60° irradiance level are shown in Figure 47. The results for the 60°/0° irradiance level are shown in Figure 48. The results for the 60°/60° irradiance level are shown in Figure 49.

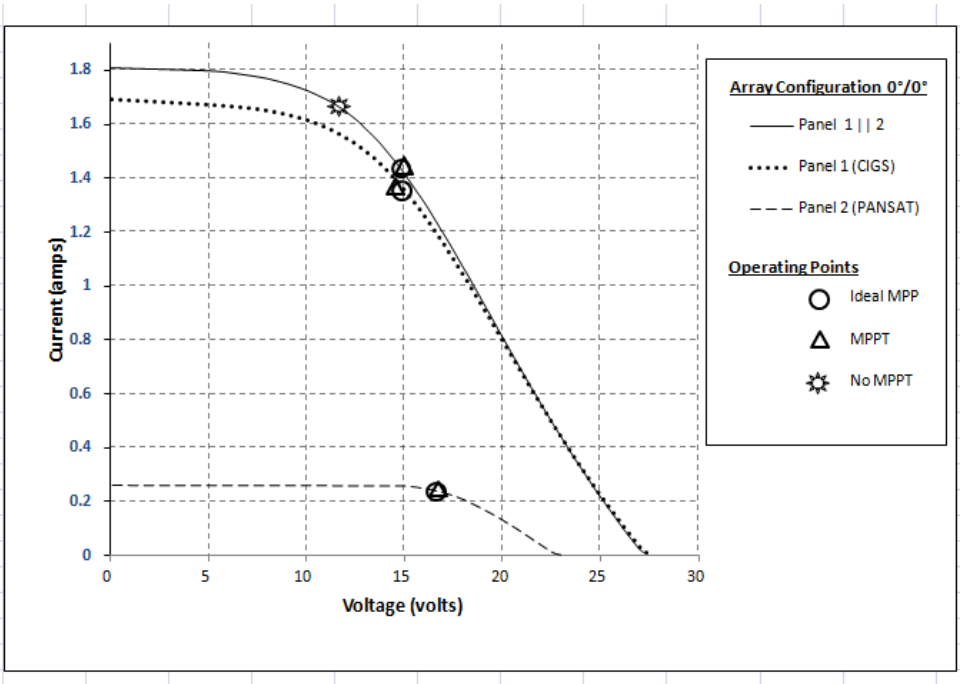

Figure 44. The I-V curves and operating points for irradiance level 0°/0°.

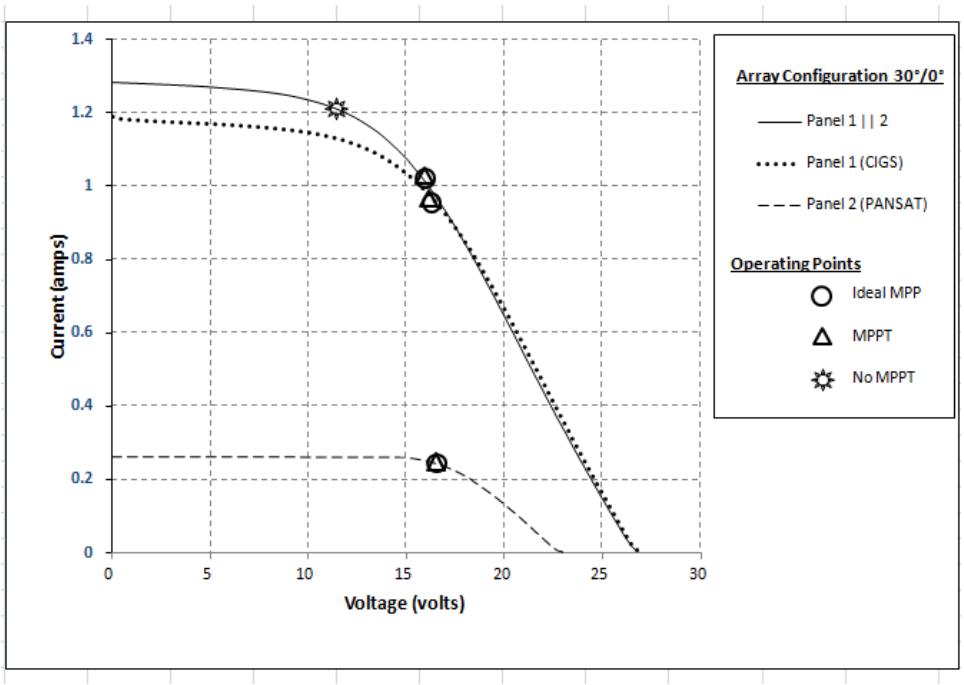

Figure 45. The I-V curves and operating points for irradiance level 30°/0°.

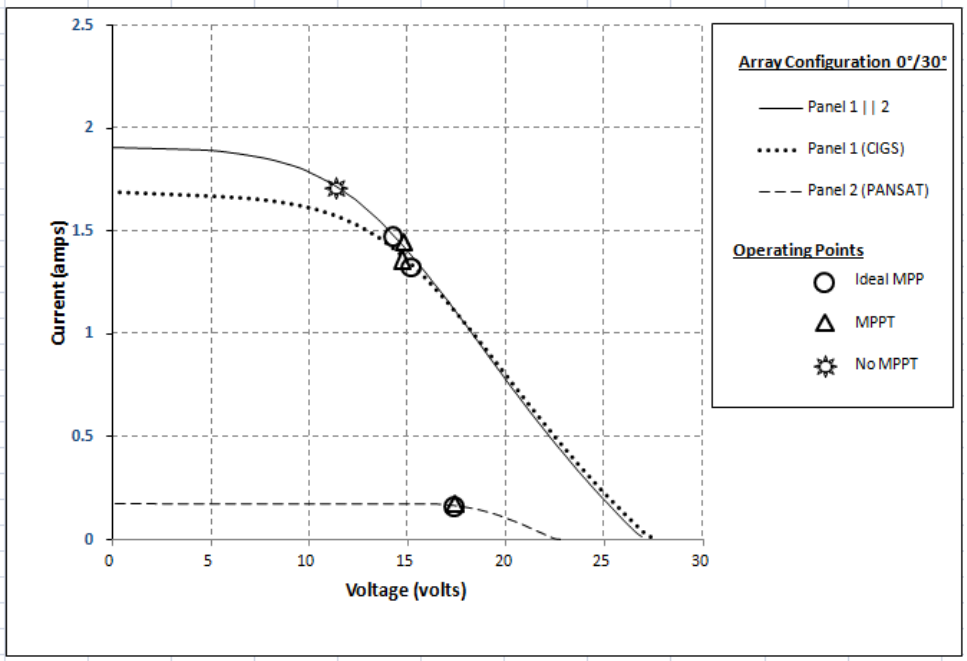

Figure 46. The I-V curves and operating points for irradiance level 0°/30°.

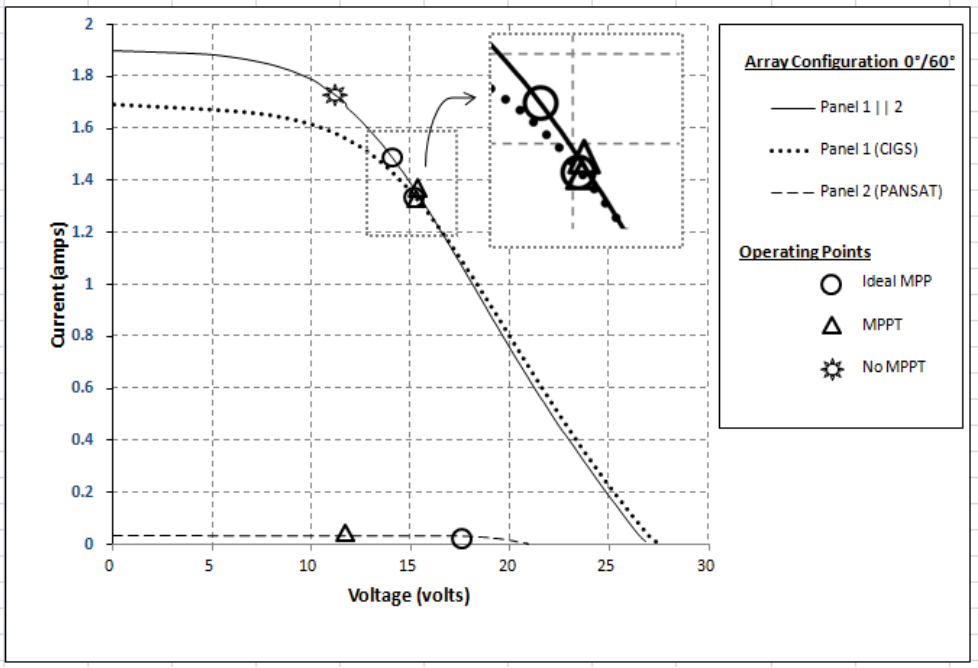

Figure 47. The I-V curves and operating points for irradiance level 0°/60°.

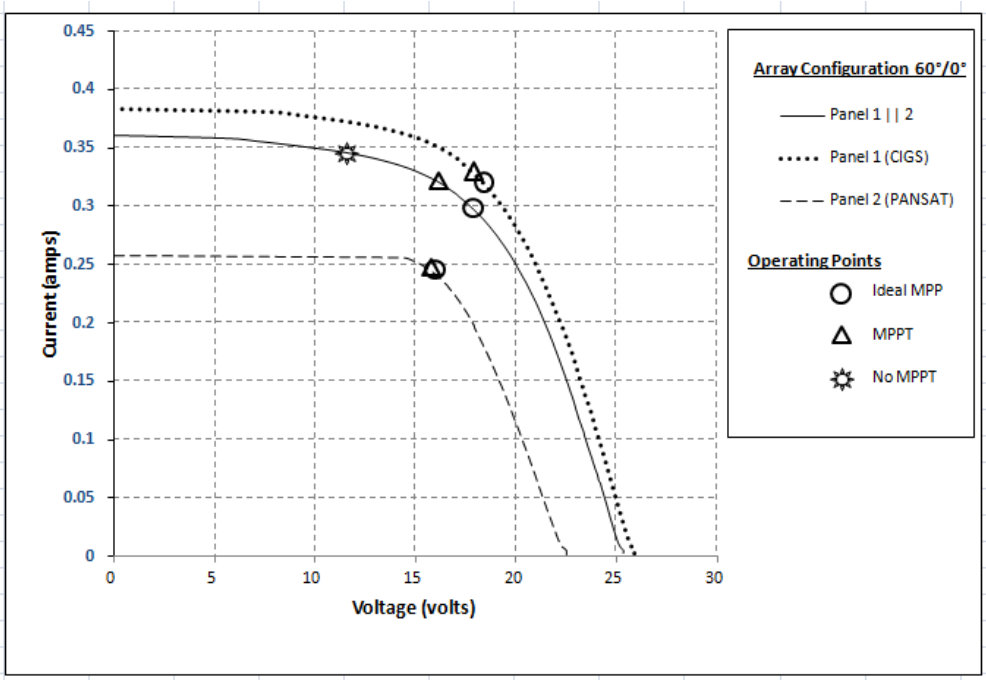

Figure 48. The I-V curves and operating points for irradiance level 60°/0°.

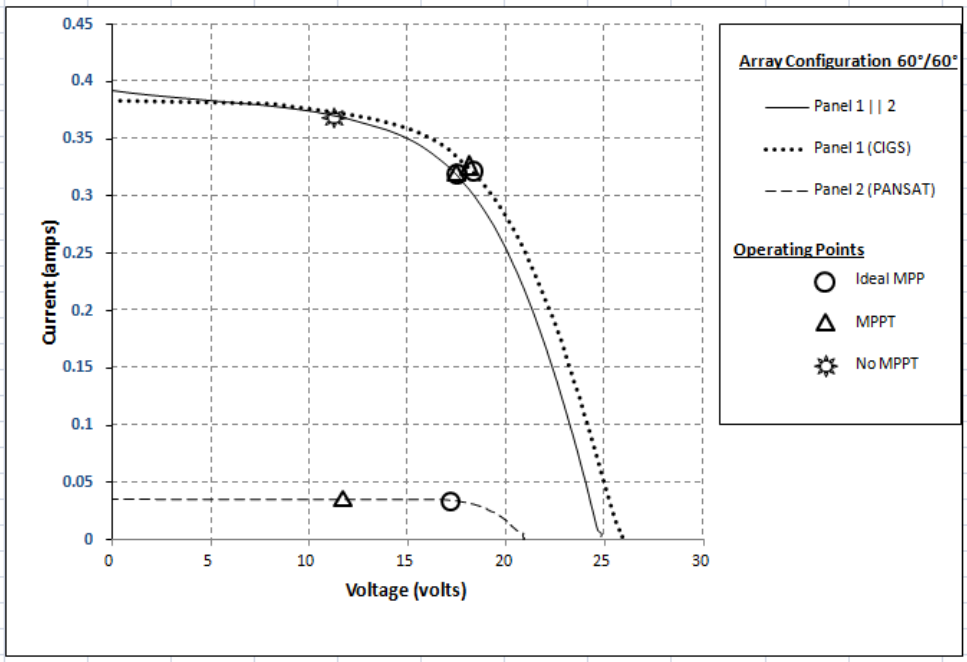

Figure 49. The I-V curves and operating points for irradiation level 60°/60°.

LIST OF REFERENCES

[1] B. Betz. (2012, September 5). *PV microinverters and power optimizers set for significant growth* [PV Magazine Online]. Available: http://www.pv-magazine.com/news/details/beitrag/pv-microinverters-and-power-optimizers-set-for-significant-growth_100008296/#axzz26lVQcSs7

[2] D. Hettelsater, et al. (2002, May 2). *Lab 7: solar cells* [Online]. Available: http://classes.soe.ucsc.edu/ee145/Spring02/EE145Lab7.pdf

[3] A. D. Gleue. (2008, June). *The basics of a photovoltaic solar cell* [Online]. Available: http://teachers.usd497.org/agleue/Gratzel_solar_cell%20assets/Basics%20of%20a%20Photovoltaic%20%20Solar%20Cell.htm

[4] R. M. Fernadez, Jr., "A novel photovoltaic power converter for military and space applications," M.S. thesis, Dept. Electron. Eng., Naval Postgraduate School, Monterey, California, 2005.

[5] *Solar Electricity Handbook: Solar Irradiance*. Greenstream Publishing, Warwickshire, United Kingdom, 2009 [Online]. Available: http://solarelectricityhandbook.com/solar-irradiance.html

[6] G. Kopp and J. Lean. (2011, January 14). "A new, lower value of total solar irradiance: evidence and climate significance," in *Geophysical Research Letters* [Online], vol. 38, L01706. Available: http://www.agu.org/pubs/crossref/2011/2010GL045777.shtml

[7] S. Michael, "Solar cell basics notes for EC3230 (Space Power and Radiation Effects)," unpublished, Naval Postgraduate School, Monterey, California.

[8] M. Berrera et al., "Experimental test of seven widely-adopted MPPT algorithms," in *IEEE Power Tech Conf.*, Budapest, Hungary, 2009.

[9] J.Jiang et al., "Maximum power point tracking for PV power systems," in *Tamkang Journal of Science and Engineering*, Vol. 8, No. 2, 2005 pp. 147–153.

[10] D. P. Hohm and M. E. Ropp, "Comparative study of maximum power point tracking algorithms," in *Progress in Photovoltaics: Research and Applications*, Vol. 11, Issue 1, 2003, pp. 47–62.

[11] J. Ahmad, "A fractional open circuit voltage based MPPT for PV arrays," in *IEEE 2nd Int. Conf. on Software Technology and Engineering*, Ansan, South Korea, 2010.

[12] D. Petreus et al., "A novel implementation of a maximum power point tracking system with digital control," in *IEEE Int. Sym. on Industrial Electronics*, Cluj-Napoca, Romania, 2011.

[13] Y. Jiang et al., "Load current based analog MPPT controller for PV systems," in *27th Annual Applied Power Electronics Conf. and Expo.*, Tuscaloosa, AL, 2012.

[14] N. Femia et al., "A new analog MPPT technique: TEODI," in *IEEE Progress in Photovoltaics: Research and Applications*, Vol. 18, 2010, pp.28–41.

[15] S. Kim and G. Rincon-Mora, "Efficiency of switched-inductor dc-dc converter ICs across process technologies," in *IEEE Explore*, 2012 [Online]. Available: http://ieeexplore.ieee.org/stamp/stamp.jsp?arnumber=06272064

[16] S. Keeping. (2012, July). *Techniques to limit switching dc/dc converter inefficiency during low loads* [Electronic Products Online]. Available: http://www.digikey.com/us/en/techzone/power/resources/articles/techniques-to-limit-switching-dc-dc-inefficiency.html

[17] M. Seeman et al., "A comparative analysis of switched-capacitor and inductor-based dc-Dc conversion Technologies," in *IEEE 12th Workshop on Control and Modeling for Power Electronics*, Urbana, IL, 2010.

[18] Wikipedia. (2012, November 8). ***PV microinverters*** [Online]. Available: http://en.wikipedia.org/wiki/Solar_micro-inverter

[19] R. Muenster. (2009, February 2). ***Shade happens*** [National Semiconductor Online]. Available: http://www.renewableenergyworld.com/rea/news/article/2009/02/shade-happens-54551

[20] ENPHASE. (2012, November 9). ***Micro-inverter energy performance analysis*** [Online]. Available: http://enphase.com/wp-uploads/enphase.com/2011/08/Enphase-Handout-Performance-versus-PVWatts.pdf

[21] K. Dolan, "Enphase's rooftop solar revolution," in ***Forbes Magazine***, November 2010.

[22] S. Michael, "Satellite configuration notes for EC3230 (space power and radiation effects)" unpublished, Naval Postgraduate School, Monterey, California.

[23] H. Kenyon, "Off-the-shelf gear strengthens Marine operations," in ***Signal Magazine***, April 2010.

[24] C. Chin, "Extending the endurance, missions and capabilities of most UAVs, using advanced flexible/ridged solar cells and using new high power density batteries technology," M.S. thesis, Dept. Electron. Eng., Naval Postgraduate School, Monterey, California, 2011.

[25] R. Phelps, "Safe operation of RST solar simulator, version 2," unpublished, Space Systems Academic Group, Naval Postgraduate School, Monterey, California.

[26] ***Designing with the SPV1020, an interleaved boost converter with MPPT algorithm***, Steval USA, Boca Raton, FL, 2012.

THIS PAGE INTENTIONALLY LEFT BLANK

INITIAL DISTRIBUTION LIST

1. Defense Technical Information Center
   Ft. Belvoir, Virginia

2. Dudley Knox Library
   Naval Postgraduate School
   Monterey, California

3. Marine Corps Representative
   Naval Postgraduate School
   Monterey, California

4. Professor Clark Robertson, Chairman
   Department of Electrical and Computer Engineering
   Naval Postgraduate School
   Monterey, California

5. Professor Sherif Michael
   Department of Electrical and Computer Engineering
   Naval Postgraduate School
   Monterey, California

6. Professor Robert Ashton
   Department of Electrical and Computer Engineering
   Naval Postgraduate School
   Monterey, California

7. Director, Training and Education, MCCDC, Code C46
   Quantico, Virginia

8. Director, Marine Corps Research Center, MCCDC,
   Code C40RC
   Quantico, Virginia

9. Marine Corps Tactical Systems Support Activity
   (Attn: Operations Officer)
   Camp Pendleton, California

10. Christopher Stephenson
    Murfreesboro, Tennessee